We thank all the reviewers for their valuable comments, which have greatly contributed to improving the quality of the manuscript. Our point-by-point responses (**blue**) and the proposed changes to the manuscript (**red**) are embedded below within the referees' original comments (**black**). For cases where the changes are substantial throughout the entire manuscript, we refer to the revised manuscript (with track changes) attached at the end of this response.

Authors' Response to Anonymous Referee #1

The manuscript presents measurements of the organic/elemental carbon fractions and optical properties (scattering, absorption, extinction) of aircraft engine soot sampled at the exhaust plane of the engine while in a ground-based test cell. Four different fuels were examined, including both Jet A-1 and mixtures of Jet A-1 with a HEFA jet biofuel. The manuscript is relatively short and well written. There is a quite a bit of methods information in the supplementary material that should be moved to the main text to improve readability. The paper should be publishable after the following comments are addressed:

R1.1) Referee comment:

1) Emissions data are reported in terms of concentrations (e.g., mg m^{-3} or Mm^{-1}), which are not particularly informative to the reader for interpreting the differences between thrust settings and fuels. The authors should normalize the results using the CO2 concentration data to report the data in terms of emissions indices (e.g., mg [kg fuel]$^{-1}$ for mass emissions and m^2 [kg fuel]$^{-1}$ for optical coefficients). While this makes the data more useful and accessible to the readers, it won't change the intensive parameters, and therefore the conclusions of the paper.

Author's response:

We see the benefit of fuel normalized emissions, in particular for PM mass and EC. However, we do not believe that the normalization of optical data with fuel consumption would make the data more accessible and we think that such a normalization might confuse some readers. However, in order to make our results readily available for the modelling community, we have added in the supplementary information the thrust and fuel dependent emission index (EI) of EC ($EI_{m,EC}$), all the additional data needed to calculate EIs (i.e. CO_2, CO and THC concentrations) and the particles' size data (GMD and GSD). Therefore, fuel-normalized optical coefficients can easily be determined if needed and the data becomes more accessible.

Changes in text:

Page 8, Line 13: The EC, OC and TC mass concentrations are reported in Table S3. Additionally, in Table S4 we also report the mass emission index of EC ($EI_{m,EC}$, in mg kg_{fuel}^{-1}), together with the additional parameters required for the calculation of EIs (i.e. carbon dioxide, carbon monoxide and hydrocarbon concentrations) and the particles' size parameters (geometric mean diameter (GMD) and geometric standard deviation (GSD)).

	Thrust (%)	CO_2 * (ppm)	CO ** (ppm)	THC (ppm)	$EI_{m,EC}$ (mg kg_{fuel}^{-1})	GMD (nm)	GSD (nm)
Jet A-1	95.6	45101.5	30.4	16.4	166.4 ± 11.8	42.4 ± 0.6	1.91 ± 0.05
	77.4	40793.8	17.2	9.1	119.8 ± 8.0	36.5 ± 0.3	2.02 ± 0.04
	64.0	36546.1	14.5	12.7	93.2 ± 6.0	32.1 ± 0.2	2.10 ± 0.03
	52.7	33274.3	12.9	7.7	36.4 ± 2.4	27.0 ± 0.1	2.12 ± 0.02
	28.8	28471.7	31.2	11.0	3.3 ± 0.6	17.2 ± 0.1	1.89 ± 0.01
	5.2*	20726.1	303.6	71.6	0.9 ± 0.3	9.0 ± 0.1	1.93 ± 0.02
	2.7	23230.7	753.4	295.1	5.5 ± 0.9	7.9 ± 0.1	1.94 ± 0.02
HEFA 32%	96.2	44803.0	25.0	9.7	141.5 ± 9.2	40.1 ± 0.4	1.98 ± 0.04
	96.0	44170.7	22.2	10.2	141.9 ± 9.3	38.4 ± 0.4	2.02 ± 0.04
	94.2	44459.0	27.1	10.2	149.3 ± 10.7	39.1 ± 0.5	1.99 ± 0.05
	85.1	41531.6	19.0	9.0	122.6 ± 8.0	35.9 ± 0.3	2.04 ± 0.04
	83.2	41559.1	17.7	9.0	120.9 ± 7.9	36.6 ± 0.2	2.06 ± 0.03
	63.3	36323.7	13.4	8.0	70.9 ± 4.5	30.1 ± 0.2	2.13 ± 0.03
	62.5	36160.0	13.8	7.8	63.8 ± 4.1	29.5 ± 0.2	2.17 ± 0.03
	29.3	28237.1	28.3	7.8	1.7 ± 0.4	15.2 ± 0.1	1.84 ± 0.01
	2.8	22969.8	769.7	306.2	2.6 ± 1.1	6.6 ± 0.1	2.06 ± 0.02

* CO_2 measured in the PM line corrected for dilution; ** CO corrected for wet measurement conditions

Table S4. Thrust and fuel dependent CO_2, CO and THC concentrations for the calculation on emission indexes, calculated emission index of EC ($EI_{m,EC}$), and particles size parameters (GMD and GSD) obtained from the fit of the size distributions.

R1.2) Referee comment:

2) It would be worthwhile to split the panels in Figures 2 and 3 into multiple figures that emphasize key relationships in the analysis. For example: 1) a new figure combining Figures 2d and 2e with Figure 3d to emphasize the MAC calculations and the contribution of EC and OC to the MSS BC mass EI. Similarly, a new figure combining Figure 2f and Figure 3f emphasizes the transition at ~50% thrust from highly scattering, organic carbon-dominated exhaust particles to highly absorbing, elemental-carbon-dominated exhaust particles. I would encourage the authors to think critically about how best to present these figures in order to support their discussion rather than just lump them into large, multi-panel figures with different (and not really comparable) x-axes.

Author's response:

We thank the reviewer for his/her suggestion. Following his/her recommendation we have divided Figs. 2 and 3 into 5 different figures and have restructured/adapted the results and conclusions sections accordingly. The results section in the revised manuscript is divided in the following sections/figures:

3.1 Chemical composition → Fig. 2: EC, OC and TC thrust dependency + HEFA decrease
→ Fig. 3: EC and OC correlations with BC_{MSS}

3.2 Optical properties → Fig. 4: b_{abs}, b_{scat} and b_{ext} thrust dependency
→ Fig. 5: b_{abs} vs EC (determination of MAC values)

3.3 Link between chemical composition and optical properties → Fig. 6: OC/TC and SSA thrust dependency

3.4 Radiative properties

Changes in text:

See revised manuscript (with track changes) at the end of this response.

R1.3) Referee comment:

3) The article is rather short as it is currently structured, so much of the additional discussion in the supplementary material could and should be moved to the main text. This is particularly true of the text in Section S1. The tables and figures in Section S1 could remain in the supplementary material with direct referencing from the main manuscript. Section S1.4, in particular, is rather theoretical, speaks to the measurement data quality, and would be valuable to placed in the more prominent location of the main manuscript.

Author's response:

Although we agree with the reviewer that some of the sections in the supplementary material contain important information (regarding for example instruments calibration and validation of the measurements), we believe that moving such detailed descriptions of experimental procedures to the main text could decrease the level of attention given to the main findings of the work. In particular:

- Section S1.1 contains details of the experimental setup that are not unique to this work and have already been reported in previous publications.
- Section S1.2 contains a detailed description of the methodology for EC/OC analysis. This is a standard methodology and therefore its description in the main text is not required.
- Section S1.3 contains the laboratory calibrations of the CAPS and PAX. Again, those are mainly standard procedures that therefore do not need to be described in detail in the main text.
- Section S1.4 contains the comparisons between laboratory calibration measurements and the estimates from Mie theory. These comparisons were performed as a data quality check, after some inconsistencies had been found in the NO_2 interference calibration for the CAPS instrument. Although the section is rather extensive, the only important outcome is that our CAPS scattering signal is hampered and was therefore not used in our analysis. As this is not an instrumental manuscript, we believe that including this full section to the main text would just add unnecessary complexity to the manuscript, and reporting the main findings of the comparison is enough in order to assess the data quality in the main text.
- Section S1.5 is a consequence of the results of Section S1.4 and briefly shows how we estimated the scattering coefficient at 532 nm. As for the Section S1.4, we think that adding a detailed description of this calculation in the main manuscript is not necessary.

As mentioned above, sections S1.3, S1.4 and S1.5 are of great importance for the assessment of the data quality. However, we do not think that the manuscript would benefit from a very detailed description of these sections in the main text. Instead, we only briefly introduce the measurements and main findings of each section with appropriate references to the supplementary information, so that readers that are interested in the detailed methods and procedures can easily access them.

R1.4) Referee comment:

4) I agree with the other reviewers that the simplified radiative forcing model and calculations presented in Section 3.3 do not really add much to the paper. This is evident from the merely qualitative discussion of this section in the abstract and conclusions. One would expect a priori that introducing absorbing aerosols such as aircraft soot above a reflective surface would produce a warming effect and that the magnitude of this warming effect would decrease over darker surface types. I suggest that this section be removed.

Author's response:

We thank the reviewer for his suggestion. Our goal of reporting the simple forcing efficiency was to put the determined MAC, MSC and SSA into context, by using them in a simple radiative transfer model. However, we agree with the reviewer that using this simple model without considering the plume evolution processes (which is out of the scope of this work and drastically affects the light

scattering and SSA) does not add significant value to the manuscript and the presented results could be misunderstood. Following the reviewers suggestion regarding the split of Figs. 2 and 3, we have substantially restructured the results section in the revised manuscript (see track changes below). The section "Radiative forcing" has been changed to "Radiative properties" and focuses on the determination and discussion of the MAC and MSC values. The main description of the model and its results have been moved to the supplementary information, and only the main outcomes are briefly presented at the end of this new section. In addition, at every occasion where the model results are mentioned, we explicitly note that these results are only representative of fresh emissions, while more complex models and plume evolution measurements would be required to assess the overall radiative effects of aircraft PM emissions.

Changes in text:

See revised manuscript (with track changes) at the end of this response.

Authors' Response to Anonymous Referee #2

The manuscript "Chemical composition, optical properties and radiative forcing efficiency of nascent particulate matter emitted by an aircraft turbofan burning conventional and alternative fuels" describes test rig measurements on a CFM56 engine using a series of different HEFA blends. Particles in the engine exhaust were characterized with filter OC/EC measurements and PAX/CAPS instruments. The results were used to estimate the radiative forcing of the particles in the atmosphere.

R2.1) Referee comment:

The manuscript covers a topic of current scientific interest and the experimental details are sound. However, some assumptions with regard to the radiative forcing are rather bold. It is presumed that that the particles at the engine exit plane on a test rig are similar to particles behind the engines inflight. It is not clear to me if the authors considered changes to the particles in the contrails. The authors do not discuss limitations of their study but I think this is vital for the manuscript.

Author's response:

This is a good point raised by the reviewer that needs some clarifications. The main limitations of our study are discussed at the beginning of the results section (Page 7, Line 30). While we are aware of the limitations associated to the ground measurements at the engine exit plane, the main goal of this manuscript is to report the major optical parameters of fresh aircraft PM emissions for different thrust levels and fuel types, as these are scarce in the literature and valuable for modelling studies. In the revised manuscript we have clarified how the temperature and pressure differences between ground and cruise altitude measurements can be assumed to have a negligible effect on the optical properties of the emissions. The results of a simple radiative forcing model are presented merely to put the obtained radiative properties (MAC, MSC and SSA) into context and illustrate that aircraft fresh emissions can have a significant radiative effect under certain conditions (e.g. emissions over high albedo surfaces). However, as we discuss in the manuscript, the atmospheric aging of the particles in the emission plume will affect their radiative properties, which can largely differ from those of the direct fresh emissions reported in this work. Further experimental work (plume evolution measurements) and more complex modelling studies are required to properly evaluate the plume evolution of aircraft emissions in the atmosphere and the associated radiative forcing. However, such experimental efforts are out of the scope of this manuscript. These considerations have been highlighted in the revised manuscript.

Changes in text:

Page 7, Line 29: Some additional considerations are needed regarding the representativeness of the data presented in this work. First, our results characterize the emissions at the engine exit plane from an engine operated ~~on~~ at the ground. Thus, a correction to take into account the atmospheric conditions (temperature and pressure) at flight altitude is in principle necessary. However, as shown in Durdina et al. (2017) using data from a turbofan engine representative of modern commercial~~ly~~ engines (Howard et al., 1996), the altitude does not significantly influence the PM

size distributions. While ambient conditions will affect the plume evolution, the effect on the PM chemistry at the engine exit plane can be assumed to be minimal. Consequently, also the optical properties, which strongly depend on the particle size and chemical composition, would remain unvaried at the engine exit plane. Hence we ~~can~~ assume the altitude correction for the optical properties at the engine exit plane to be negligible. ~~minor as well. In addition,~~ It is important to note however, that most gaseous and particle species measured at the engine exit plane will evolve in the atmosphere and their radiative effects can largely vary from those of the direct emissions presented in this work, where the collected data correspond~~s~~ to a time after emission of approximately 0.1 to 0.6 seconds (Brem et al., 2015). Additional measurements are therefore required in order to assess the evolution of the particles' optical properties in the emission plume. ~~the plume evolution of aircraft emissions in the atmosphere.~~ In any case, the emissions at the engine exit plane are the basis to consider the evolution of PM properties and are therefore the baseline for diverse atmospheric modelling scenarios.

Page 12, Line 2: However, these results need to be taken with caution, as this simple radiative model does not consider the effect of underlying clouds. Moreover, we only consider the effect of fresh PM emissions, corresponding to an approximate time after emission of less than 0.6 s, where the jet is still conserved and high temperatures prevent the condensation of volatile species. Previous studies have shown that sulfuric acid plays an important role in the formation of secondary PM in near-field aircraft plumes (Kärcher et al., 1996). Thus, plume evolution measurements of the particles' optical properties (if possible in-flight) and more complex models are needed to assess the overall radiative effects of aircraft PM emissions.

Page 14, Line 5: However, more accurate and complex climate models that simulate the atmospheric aging of the particles in the emission plume and take into account the effect from variable underlying cloud fields are required for a complete understanding of the impact of aviation particle emissions on the Earth's radiative balance.

R2.2) Referee comment:

With regard to the impact of the HEFA blends, the authors conclude that "the particles originated from the combustion seem to be equivalent in terms of their normalized optical properties and only their concentration change" (page 11). Huang et al. analyzed the particle morphology in the APEX III campaign. They conclude that "Such dependence upon combustion indicates that PM from alternative fuels will be different from that by JP-8. Models of PM formation in turbulent reaction environments will need to include such variations for accurate prediction. Accordingly optical properties and surface chemistry will vary too." (Huang, C.H., Bryg, V.M., Vander Wal, R.L., 2016. A survey of jet aircraft PM by TEM in APEX III. Atmospheric Environment 140, 614-622).This finding does not fit to the statement in the current manuscript. The authors are recommended to discuss this discrepancy and the uncertainty of their findings.

Author's response:

Our results show that the use of a 32 % vol. HEFA- Jet A-1 blend does not significantly influence the intensive optical properties of the emitted particles (SSA, MAC or MSC), compared to standard Jet A-1. These results are supported by the observations on the OC/TC fraction, which is directly linked to the SSA, and is also found to be independent of the type of fuel burned.

The statement in the manuscript of Huang et al. pointed out by the reviewer refers to pure alternative fuels, and does might hold for the blends of alternative fuel with Jet A-1 used in our work. The fuel effects on soot morphology were studied during the AAFEX II measurement campaign, where 4 fuel types were tested: JP-8 (similar to Jet A-1), FT (Fischer-Tropsch), HRJ (hydro-treated renewable jet), and a 50:50 blend of JP-8 and HRJ. The results, presented in Huang and Vander Wal (2013), show that due to the aromatic content in the JP-8 fuel, the soot formation starts earlier (lower temperatures) than for the synthetic fuels (FT and HRJ) that are mainly paraffinic in content (higher smoke point). The required pyrolysis reactions that delay soot formation in the case of alternative fuels, allow for greater partial premixing to occur (via turbulent mixing) compared to the JP-8. This explains the differences in the nanostructures observed form the combustion of these fuels, e.g.: at low thrust, particle cores from JP-8 lack internal structure and have high organic content while particles from FT and HRJ fuels have a clear visible core structure. In addition, for JP-8 fuel the soot nanostructure varied with engine power level (linked to the high aromatic content of the fuel and changes in the local chemical environment), while for the alternative fuels distinct and varied types of nanostructures were found irrespective of engine

operating conditions. Accordingly, the differences between JP-8 fuel and the pure alternative fuels (FT and HRJ) could cause significant differences in the optical properties of the emitted particles, but this is not necessarily the case for the blends of alternative fuel with base fuel. In fact, the 50:50 blend of JP-8 and HRJ in the work of Huang and Vander Wal (2013) exhibits a similar trend of soot nanostructure evolution to that of the JP-8 fuel. In our work we use an even lower level of alternative fuel blending (max. 32 % HEFA), which can explain why we do not observe significant differences in the optical properties of the particles emitted when burning Jet A-1 fuel and the HEFA blends. A summary of this discussion will be added in the revised manuscript (see below).

Changes in text:

Page 13, Line 24: Previous works found significant differences in the morphology of the particles emitted when burning pure alternative fuels compared to standard jet fuels, which would translate into major differences in the particles' optical properties (Huang and Vander Wal, 2013; Huang et al., 2016). However, this does not seem to be the case for blends of alternative fuels at practical ratios for widespread usage in the foreseeable future and with considerable (> 8% v/v) total aromatics content. In fact, Huang and Vander Wal (2013) found similar trends in the soot nanostructure evolution with thrust for standard jet fuel and its 50:50 blend with an alternative fuel, while the two pure biofuels tested produced distinct and varied types of nanostructures independent of the engine thrust. Huang and Vander Wal (2013) related these differences to the different degrees of turbulent mixing in the combustion chamber prior to soot formation, which is linked to the aromatic content in the fuel. Thus, soot formation from blends with up to 50% of alternative fuel is fairly similar to the one of the unblended base fuel, which results in emissions of soot particles with similar morphology, OC/TC ratios and intensive optical properties.

R2.3) Referee comment:

Overall, estimating the global impact of particles in the atmosphere based on one ground measurement of an in-service engine might be not valid enough. Nevertheless, the fuel variation experiment and its results are important for the current discussion of extended use of alternative fuels in aviation.

Author's response:

We fully agree with the reviewer that for a precise estimate of the global impact of aircraft emitted particles, additional measurements, including different engine types and plume evolution studies, are needed. Such measurements are however hindered by their high costs, e.g. for the measurements presented in this work 103 tons of fuel were burnt and 700+ working hours were invested. As discussed above, the simple radiative transfer model used in this work for engine exit plane emissions is aimed only to illustrate the potential radiative efficiency of fresh particle emissions over different surface types, but more complex models that take into account the physico-chemical evolution of the particles after emission are essential for a proper estimate of the radiative forcing of aircraft PM emissions. In the revised manuscript the section "Radiative forcing" has been changed to "Radiative properties" and focuses on the determination and discussion of the MAC and MSC values. The main description of the simple radiative model and its results have been moved to the supplementary information, and only the main outcomes are briefly presented at the end of this new section (see track changes in the manuscript).

Authors' Response to Anonymous Referee #3

This paper provides details of the chemical composition and the optical properties of the particulate matter (PM) measured at the exit plane of a CFM56-7B engine burning four blends of Jet A-1 and HEFA fuels. The paper itself is an important contribution to the literature in terms of characterizing the chemical and optical properties from an aircraft engine burning fuels with varying composition. The paper is well written but has several deficiencies that must be addressed by the authors. Chief among them is how the authors calculate the direct radiative forcing.

General Comments:

R3.1) Referee comment:

The measurements reported in this paper were performed at ground level behind the engine exit plane, but the authors have not adequately discussed the impact of different temperature and pressure regimes at cruise levels on optical properties.

Author's response:

This comment has been addressed above as part of the response to R2.1.

R3.2) Referee comment:

Also, the impact of plume evolution at cruise conditions had not been discussed. The authors' goal of coming up with radiative effect of aircraft particulate emissions falls short in this regard.

Author's response:

The main goal of this manuscript is to report the major optical parameters of fresh aircraft PM emissions for different thrust levels and fuel types, as these are scarce in literature and of great value for atmospheric modelling studies. The results of the simple radiative forcing model were presented merely to give an idea of the radiative effect of fresh (0.1 to 0.6 seconds after emissions) aircraft aerosol emissions occurring over different surface types (i.e. albedos). As we discuss in the manuscript, the atmospheric aging of the particles in the emission plume will affect their radiative properties (as well as morphology, size, composition…), which can largely differ from those of the direct fresh emissions reported in this work. To properly evaluate the radiative effects of the particles in the emission plume, considerable experimental work (plume evolution measurements including optical properties, if possible in-flight) and/or much more complex modelling studies are needed. Such experimental efforts were out of the scope of this manuscript. We have instead modified the manuscript to further stress that the modelling results correspond to fresh emissions and are not representative of the effects from aged aircraft emissions. We have also restructured the results section, highlighting the discussion of the retrieved radiative properties (in terms of MAC, MSC and SSA) and moving most of the modelling results to the supplementary information

Changes in text:

See revised manuscript (with track changes) at the end of this response.

Specific comments:

R3.3) Referee comment:

Pg 1, Ln 3: The authors switch between "aircraft particulate emissions" and "aircraft exhaust aerosol". Please be specific and consistent.

Author's response:

We thank the reviewer for pointing out this inconsistency. In the revised manuscript we have replaced "aircraft particulate emissions" with "aircraft exhaust aerosol", as the latter specifies that we refer to emissions from aircraft engines.

Changes in text:

Page 1, Line 16: Due to the lack of measurement data, the radiative forcing from aircraft exhaust aerosol ~~particulate emissions~~ remains uncertain.

R3.4) Referee comment:

Pg 1, Ln 19: I'm not sure what "The separation of elemental carbon (EC) and organic carbon (OC)" means? Please clarify

Author's response:

We refer to the thermal separation of the total carbon sampled on a filter into elemental and organic carbon. Although the term "separation" is widely used in this context, we will replace it in the revised manuscript to avoid confusion.

Changes in text:

Page 1, Line 23: The analysis ~~separation~~ of elemental carbon (EC) and organic carbon (OC) revealed a significant mass fraction of OC (up to 90%) at low thrust levels, while

Page 4, Line 5: The chemical characterization of the exhaust was based on the quantification ~~separation~~ of elemental and organic carbon (EC/OC analysis) from filter samples…

R3.5) Referee comment:

Pg 3, Ln 25-26: Moore et al., 2017 reports on the emissions from a 50:50 blend at cruise. Please update the text to include the engine type and fuel since you have previously stated that these are important factors. Please also state that the reductions were measured at cruise levels.

Author's response:

We thank the reviewer for his suggestion. We have added the missing information in the revised manuscript.

Changes in text:

Page 3, Line 31: Moreover, a recent study on in-flight cruise emissions from the NASA DC-8 turbofan engines (CFM56-2-C1) has shown that using a 50:50 blend of Jet A and a Camelina-based HEFA biofuel ~~biofuel blends to power aircraft engines~~ reduces the ~~their~~ particle emissions by 50 - 70% (Moore et al., 2017).

R3.6) Referee comment:

Pg 3, Ln 28-29: The authors mention the engine type in the abstract. It should also be included here.

Author's response:

We have added this information in the revised manuscript.

Changes in text:

Page 4, Line 1: In this work we study the link between the chemical composition and the optical properties of the PM measured at the engine exit plane of a CFM56-7B turbofan ~~from aircraft exhaust~~ for different engine loads and HEFA fuel blends.

R3.7) Referee comment:

Pg 7, Ln 7-10: I don't see how you can assume that the difference in optical properties at altitude compared to ground level conditions are minor when you don't have any supporting evidence. Also, the study cited was for PM size distributions, and not nvPM size distributions.

Author's response:

This comment has been addressed above as part of the response to R2.1. In addition, note that our optical and EC/OC measurements are relative to the total PM emissions (only the MSS measurements are limited to the nvPM fraction). Thus, it is reasonable to consider the changes in the PM size distributions as a base to assess changes in the optical properties and the chemical composition of the emissions.

R3.8) Referee comment:

Pg 7, Ln 13-14: The authors state "Additional measurements are therefore required in order to assess the plume evolution of aircraft emissions in the atmosphere." However, there are several studies that have reported plume evolution of aircraft engine emissions. These studies have shown a dramatic change in PM size distributions from exit plane measurements. How do the authors reconcile their approach with this published literature data?

Author's response:

The aging of the particles in the emission plume will have a strong effect on the particles' size, morphology, composition, as well as on their radiative effects. Plume evolution experiments are a powerful tool to investigate such changes, but due to the very high costs of performing such measurements (especially in-flight), the amount of data reported in the literature is limited. To the best of our knowledge, this is the first work that includes a detailed characterization of the optical properties of the aircraft emissions, which is crucial to the study of the radiative effects. Although we only report the data for fresh emissions, this is the starting point for considering the aging processes. The data presented in this work should be complemented with additional measurements

of the plume evolution of the particles' optical properties and/or models to simulate the atmospheric aging of the fresh emissions and determine the radiative effects of emissions in the plume. As mentioned above, we have modified the manuscript to underline that our modelling results correspond only to fresh emissions and are not representative for aged aircraft emissions (revised manuscript with track changes at the end of this response). In addition we have also adapted the statement pointed out by the reviewer to clarify that complimentary measurements of plume evolution should include a detailed characterization of the particles' optical properties.

Changes in text:

Page 8, Line 9: Additional measurements are therefore required in order to assess the evolution of the particles' optical properties in the emission plume. ~~the plume evolution of aircraft emissions in the atmosphere.~~

R3.9) Referee comment:

Pg 8, Ln 22-23: "the decrease due to the 32% HEFA blend was highest at low thrust levels". Other studies have also reported that the largest decrease was observed at low thrust levels. Can the authors comment on why this is generally the case?

Author's response:

As the reviewer points out this is a commonly observed behavior of rich quench lean combustors which are employed in most engines. A detailed explanation is out of the scope of this work. In simple words it can be stated that aromatic structures present in the fuel serve as the initial building blocks in the soot formation pathways at low thrust. At high thrust the high temperatures and pressures (in addition to the low air to fuel ratio) synthesize aromatic structures from fuel aliphatic species and therefore fuel chemistry is less important. A more detailed explanation on this can be found in Brem et al. 2015.

Changes in text:

Page 8, Line 28: The HEFA effect was strongest at low thrust levels, inducing a decrease in EC mass of 50-60% for thrust levels up to 30%. An explanation for this thrust dependence can be found in Brem et al. (2015).

R3.10) Referee comment:

Pg 8, Ln 27-33: Can the authors put the SSA results in context with measurements from other combustion sources?

Author's response:

Following the reviewer's suggestion we have added examples of typical SSA values reported in literature for biomass burning and traffic emissions.

Changes in text:

Page 10, Line 13: The high OC content of the particles at low thrust levels resulted in very high SSA, which showed a maximum at ground idle ($SSA_{~~CAPS~~532,base}$ = 0.88 and $SSA_{~~PAX~~870,base}$ = 0.55). Such high SSA values are common of particle emissions from biomass burning at low combustion efficiency (e.g. SSA_{532nm}~0.95 in wildfire emissions (Liu et al., 2014)). The SSA decreased sharply between 30% and 60% thrust, likely due to decreasing OC fraction, ~~(Fig. 2f). The SSA was lowest~~ reaching a minimum at the combustor inlet temperatures and air/fuel ratios representative of cruise thrust (~60% thrust), where $SSA_{~~CAPS~~532,base}$ = 0.29 and $SSA_{~~PAX~~870,base}$ = 0.07. These low SSA values are characteristic of primary on-road vehicle particle emissions (e.g. 0.22 < SSA_{675} < 0.36 from tunnel measurements (Strawa et al., 2010)).

R3.11) Referee comment:

Pg 9, Ln 23-24: Diesel engine emissions are significantly different from those of aircraft engines, in terms of size, density, EC/TC, etc. Is there a more appropriate source to estimate backscattering?

Author's response:

We thank the reviewer for bringing up this important point. Measurements of the backscattering fraction (β) are quite rare in the literature and, to the best of our knowledge, they have never been reported for aviation emissions. Our choice of β was originally based on the similarities between

the SSA (or EC/TC ratios) of the particle emissions from the diesel engine (SSA_{550nm}=0.20 (Schnaiter et al., 2003)) and the aircraft engine at cruise conditions (SSA_{532nm}=0.29, this work). However, the key variable influencing the backscattering properties is the particle size, while chemical composition seems to be less important. As the particles emitted from aircraft engines are generally much smaller than those from diesel engines, our initial assumption of β might be incorrect. Therefore, we performed a rough estimate of β for aircraft fresh emissions using Mie theory. For these calculations we used the size parameters measured at cruise conditions for pure Jet A-1 fuel (GMD=29.6 and GSD=2.0 at 57.4% thrust) and the range of refractive indexes suggested by Bond and Bergstrom (2007) (i.e. m=1.75+0.63i to m=1.95+0.79i).This resulted in β = 0.27 ± 0.01, which was used to recalculate the forcing efficiencies in the revised manuscript. The effect of changing β from 0.17 to 0.27 on the estimated SFE was very small.

Changes in text:

Page 11, Line 8→ Moved to SI Page 15:

In absence of backscattering measurements, the backscattering fraction (β) was estimated with Mie theory, using the measured size parameters at cruise conditions for pure Jet A-1 fuel (GMD=29.6 and GSD=2.0 at 57.4% thrust) and the range of refractive indexes suggested by Bond and Bergstrom (2007) (i.e. m=1.75+0.63i to m=1.95+0.79i), which lead to β = 0.27 ± 0.01.~~was fixed to 0.17 as previously determined for highly absorbing soot (SSA = 0.2) from diesel emissions (Schnaiter et al., 2003).~~

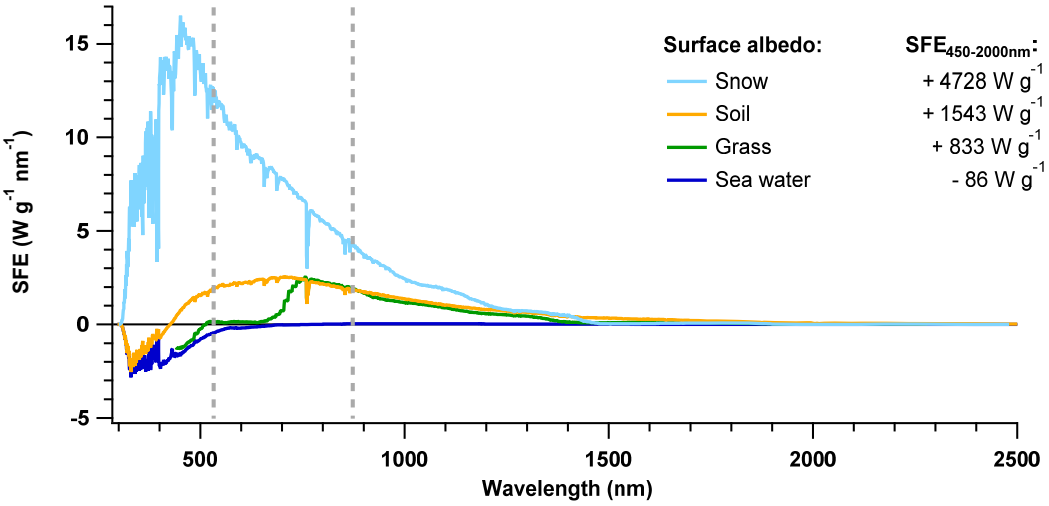

Figure S15. Simple forcing efficiency (SFE) spectra for aircraft engine PM over different surface types, including sea water, grass, soil and snow, and integrated spectral values for the four surface types.

R3.12) Referee comment:

Pg 10, Ln 8-22: The authors are using engine exit plane measurement data for SFE estimation, and do not consider the cooling effect of sulfates. This section should either be supported with additional data or removed from the paper. Also, no information is presented on the impact of using blends of HEFA with Jet A-1 on radiative forcing.

Author's response:

Our estimates of the SFE are based on the CAPS and PAX measurements, which take into account all components of the PM at the engine exit plane. As we have mentioned above, we only focus on the fresh particulate emissions at the engine exit plane, where the sulfate is only present in the gas phase. In fact, previous aerosol mass spectrometry studies performed using the same engine and sampling system have shown that inorganic nucleating species (including sulfate) are absent in the fresh conditioned exhaust of this engine (Kiliç et al., 2018; Lobo et al., 2015). Kiliç et al. also showed that the fraction of particulate sulfate (and therefore its cooling effect) becomes relevant with the plume processing in the atmosphere, but as previously mentioned, the study of the plume evolution is out of the scope of our manuscript. In the revised manuscript we have reorganized the results section in order to highlight the discussion of the radiative properties (MAC, MSC and SSA), and have moved most of the modelling results to the supplementary information. In addition, we have

clarified throughout the text that the modelling results correspond to fresh exhaust emissions and are not representative of the effects from aged aircraft emissions.

R3.13) Referee comment:

Pg 16, Table 1: It's surprising that the Jet A-1 and 10% HEFA fuels have similar hydrogen content by different aromatic contents. Since the Jet A-1 is blended with HEFA, shouldn't the hydrogen content for 10% HEFA be higher? Likewise with the 5% blend, where the hydrogen content is lower than that of the unblended Jet A-1. Can the authors explain?

Author's response:

We thank the reviewer to point this out. We have checked the values in the table and realized that the values reported corresponded to the less precise CNH method which has large uncertainties. The Table 1 has now been updated with the correct NMR values. However it has to be stated that the precision of this method is also not better than 0.1% m/m.

Changes in text:

Property (units)	Method	Jet A-1	HEFA 5%	HEFA 10%	HEFA 32%
Aromatics (% v/v)	ASTM D 1319	18.1	17.1	16.2	11.3
Naphthalenes (% v/v)	ASTM D 1840	0.79	N.A.	N.A.	0.53
Sulfur (ppm)	ASTM D 5453	490	N.A.	N.A.	350
Hydrogen mass (% m/m)	NMR	13.61~~13.8~~	13.68~~13.75~~	13.75~~13.81~~	14.09~~14.3~~
Smoke point (mm)	ASTM D 1322	22	N.A.	N.A.	24
Density (kg m^{-3})	ASTM D 4052	794.8	793.3	791.2	781.8

Table 1. Fuel specifications overview (N.A.: measurement not available)

R3.14) Referee comment:

Pg 16, Figure 1: What is APC? It has not been previously defined.

Author's response:

APC stands for Advanced Particle Counter. In the main text we decided to include only the definitions of the instruments that were used in this work. All additional instruments are defined in the supplementary information. This information has been added in the figure caption of the revised manuscript.

Changes in text:

Page 20, Line 1: Figure 1: Experimental setup during EMPAIREX 1. Instruments depicted in blue were used in this work, which included: a Micro Soot Sensor (MSS), a Cavity Attenuated Phase-Shift Single Scattering Monitor (CAPS PM_{SSA}), a Photo Acoustic Extinctiometer (DMT PAX), a Scanning Mobility Particle Sizer (SMPS), a CO_2 analyzer, a Portable Multi Gas Analyzer (PG-250), and a Chemiluminescence Detector (CLD-844). Additional instrumentation that was not used in this work (depicted in grey) is described in the supplementary information (Sect. S1.1).

R3.15) Referee comment:

Pg 17, Figure 2: Panel (f) is an interesting result (no difference in OC/TC for Jet A and 32% HEFA). Is this result unique to the fuel tested or have there been similar observations in other studies?

Author's response:

To the best of our knowledge this is the first comparison of OC/TC ratios from the combustion of Jet A1 fuel and its blends with alternative fuels. Although we do not see any significant differences in the OC/TC trends for the two fuel types, large uncertainties are associated to these values, which makes the interpretation of the results difficult. The use of biofuels has been observed to produce a stronger reduction in EC emissions than in OC emissions, leading to an increase in the OC/TC ratio. This has been reported in numerous studies of diesel engines powered with biofuels (e.g. Popovicheva et al., 2017). In our case we only observe slightly larger OC/TC ratios for the HEFA

blend at the lowest thrust levels (3-7%), but the values for the two fuel types still compare well within the large errors bars. We also see similar trends with engine thrust and fuel type in the intensive optical properties. In fact, slightly higher SSA are observed for the HEFA blend at low thrust levels (7-50%), but also the uncertainties of the SSA (ratio of two small values) are large.

The lack of significant differences in the OC/TC ratios for the two fuels might be related to the amount of biofuel mixed in the blend. Guarieiro et al. (2017) studied the morphology of the particle emissions from a diesel engine fueled with 4%, 50%, and 100% biodiesel (B4, B50, and B100, respectively), and found almost no differences in the OC/EC ratio when using the B4 and B50 fuels, while a clear increase was observed in the OC/EC ratio for the B100 biofuel. In the same line, Huang et al. (2016) studied the morphology of the particles emitted from an aircraft engine using JP-8 fuel (similar to Jet A-1), two different biofuels (FT and HRJ) and a 50:50 blend of JP-8 and HRJ. Their results show similar trends in the thrust dependent soot nanostructure resulting from the JP-8 and the 50:50 blend with HRJ, while the two pure biofuels produced distinct and varied types of nanostructures independent of the engine thrust. They relate these differences to the different degrees of turbulent mixing in the combustion chamber prior to soot formation (which is linked to the aromatic content in the fuel). Thus, blends with up to 50% of alternative fuel might follow similar combustion processes to the unblended base fuel, which results in emissions of soot particles with similar morphology and OC/EC ratios. A part of this discussion has been added in the revised manuscript.

Changes in text:

Page 13, Line 24: Previous works found significant differences in the morphology of the particles emitted when burning pure alternative fuels compared to standard jet fuels, which would translate into major differences in the particles' optical properties (Huang and Vander Wal, 2013; Huang et al., 2016). However, this does not seem to be the case for blends of alternative fuels at practical ratios for widespread usage in the foreseeable future and with considerable (> 8% v/v) total aromatics content. In fact, Huang and Vander Wal (2013) found similar trends in the soot nanostructure evolution with thrust for standard jet fuel and its 50:50 blend with an alternative fuel, while the two pure biofuels tested produced distinct and varied types of nanostructures independent of the engine thrust. Huang and Vander Wal (2013) related these differences to the different degrees of turbulent mixing in the combustion chamber prior to soot formation, which is linked to the aromatic content in the fuel. Thus, soot formation from blends with up to 50% of alternative fuel is fairly similar to the one of the unblended base fuel, which results in emissions of soot particles with similar morphology, OC/TC ratios and intensive optical properties.

References

Bond, T. C., and Bergstrom R. W.: Light absorption by carbonaceous particles: An investigative review, Aerosol Sci. Tech., 40, 27-67, doi:10.1080/02786820500421521, 2007.

Guarieiro, A. L. N., Eiguren-Fernandez, A., da Rocha, G. O., and de Andrade, J. B.: An investigation on morphology and fractal dimension of diesel and diesel-biodiesel soot agglomerates, J. Braz. Chem. Soc., 28, 1351-1362, doi:10.21577/0103-5053.20160306, 2017.

Huang, C.-H., and Vander Wal, R.L.,: Effect of soot structure evolution from commercial jet engine burning petroleum based JP-8 and synthetic HRJ and FT fuels, Energy Fuels, 27, 4946-4958, doi: 10.1021/ef400576c, 2013.

Huang, C.H., Bryg, V.M., and Vander Wal, R.L.: A survey of jet aircraft PM by TEM in APEX III, Atmos. Environ., 140, 614-622, doi:10.1016/j.atmosenv.2016.06.017, 2016.

Liu, S., Aiken, A. C., Arata, C., Dubey, M. K., Stockwell, C. E., Yokelson, R. J., Stone, E. A., Jayarathne, T., Robinson, A. L., DeMott, P. J., and Kreidenweis, S. M: Aerosol single scattering albedo dependence on biomass combustion efficiency: Laboratory and field studies, Geophys. Res. Lett., 41, 742–748, doi:10.1002/2013GL058392, 2014.

Lobo, P., Durdina, L., Smallwood, G. J., Rindlisbacher, T., Siegerist, F., Black, E.A., Yu, Z., Mensah, A. A., Hagen, D. E., Miake-Lye, R. C., Thomson, K. A., Brem, B. T., Corbin, J. C., Abegglen, M., Sierau, B., Whitefiled, P. D., and Wang, J.: Measurement of aircraft engine non-volatile PM emissions: Results of the aviation-particle regulatory instrumentation demonstration

experiment (A-PRIDE) 4 campaign, Aerosol Sci Technol., 49, 472-84, doi:10.1080/02786826.2015.1047012, 2015.

Kılıç, D., Haddad, I. E., Brem, B. T., Bruns, E., Bozzetti, C., Corbin, J., Durdina, L., Huang, R. J., Jiang, J., Klein, F., Lavi, A., Pieber, S. M., Rindlisbacher, T., Rudich, Y., Slowik, J. G., Wang, J., Baltensperger, U., and Prevot, A. S. H: Identification of secondary aerosol precursors emitted by an aircraft turbofan, Atmos. Chem. Phys., 18, 7379-91, doi:10.5194/acp-18-7379-2018, 2018.

Popovicheva, O. B., Irimiea, C., Carpentier, Y., Ortega, I. K., Kireeva, E. D., Shonija, N. K., Schwarz, J., Vojtisek-Lom, M., and Focsa, C: Chemical composition of diesel/biodiesel particulate exhaust by FTIR spectroscopy and mass spectrometry: impact of fuel and driving cycle, Aerosol Air Qual. Res., 17, 1717–1734, doi: 10.4209/aaqr.2017.04.0127, 2017.

Strawa, A., Kirchstetter, T. W., Hallar, A. G., Ban-Weiss, G. A., McLaughlin, J. R., Harley, R. A., and Lunden, M. M.: Optical and physical properties of primary on-road vehicle particle emissions and their implications for climate change, J. Aerosol Sci., 41, 36-50, doi:10.1016/j.jaerosci.2009.08.010, 2010.

Revised manuscript (with track changes):

Chemical composition~~, optical properties~~ and radiative properties~~forcing efficiency~~ of nascent particulate matter emitted by an aircraft turbofan burning conventional and alternative fuels

Miriam Elser[1,2*], Benjamin T. Brem[1**], Lukas Durdina[1***], David Schönenberger[1], Frithjof Siegerist[3], Andrea Fischer[4], Jing Wang[1,2]

[1]Laboratory for Advanced Analytical Technologies, Empa, Dübendorf, 8600, Switzerland
[2]Institute of Environmental Engineering, ETH, Zürich, 8093~~49~~, Switzerland
[3]SR Technics AG, Zurich-Airport, 8058, Switzerland
[4]Air pollution/Environmental Technology, Empa, Dübendorf, 8600, Switzerland
*now at Automotive Powertrain Technologies Laboratory, Empa, Dübendorf, 8600, Switzerland
**now at Laboratory of Atmospheric Chemistry, Paul Scherrer Institute, Villigen, 5232, Switzerland
***now at Centre for Aviation, School of Engineering, Zurich University of Applied Sciences, Winterthur, 8401, Switzerland

Correspondence to: Miriam Elser (miriam.elser@empa.ch)

Abstract. Aircraft engines are a unique source of carbonaceous aerosols in the upper troposphere. There, these particles can more efficiently interact with solar radiation than at ground. Due to the lack of measurement data, the radiative forcing from aircraft exhaust aerosol ~~particulate emissions~~ remains uncertain. To better estimate the global radiative effects of aircraft exhaust aerosol, its optical properties need to be comprehensively characterized. In this work we present the link between the chemical composition and the optical properties of the particulate matter (PM) measured at the engine exit plane of a CFM56-7B turbofan. The measurements covered a wide range of power settings (thrust), ranging from ground idle to take-off, using four different fuel blends of conventional Jet A-1 and Hydro-processed Ester and Fatty Acids (HEFA) biofuel. At the two measurement wavelengths (532 and 870 nm) and for all tested fuels, the absorption and scattering coefficients increased with thrust, as did the PM mass. The analysis ~~separation~~ of elemental carbon (EC) and organic carbon (OC) revealed a significant mass fraction of OC (up to 90%) at low thrust levels, while EC mass dominated at medium and high thrust. The use of HEFA blends induced a significant decrease in the PM mass and the optical coefficients at all thrust levels. The HEFA effect was highest at low thrust levels, where the EC mass was reduced by up to 50-60%. The variability in the chemical composition of the particles was the main reason for the strong thrust dependency of the single scattering albedo (SSA), which followed the same trend as the OC/TC fraction. Mass absorption coefficients (MAC) were determined from the correlations between aerosol light absorption and EC mass concentration. The obtained MAC values (MAC_{532} = 7.5 ± 0.3 m^2 g^{-1} and MAC_{870} = 5.2 ± 0.9 m^2 g^{-1}) are in excellent agreement with previous literature values of absorption cross section for freshly generated soot. While the MAC values were found to be independent of the thrust level and fuel type, the mass scattering coefficients (MSC) significantly varied with thrust. For cruise conditions we obtained MSC_{532} = 4.5 ± 0.4 m^2 g^{-1} and MSC_{870} = 0.54 ± 0.04 m^2 g^{-1}, which fall within the higher end of MSCs measured for fresh biomass smoke. However, the latter comparison is limited by the strong

dependency of MSC on the particles size, morphology and chemical composition. ~~The Simple Forcing Efficiency (SFE) was used to evaluate the direct radiative effect of aircraft particulate emissions for various ground surfaces. The results indicate that aircraft PM emissions over highly reflective surfaces like snow or ice have a substantial warming effect.~~ The use of the HEFA fuel blends significantly decreased PM emissions, but no changes w~~h~~ere observed in terms of EC/OC composition~~,~~ ~~optical properties~~ and radiative properties. ~~forcing per mass emitted.~~

1 Introduction

The rapid rise ~~expansion~~ of the aviation industry in the last decades and the continuous growth projected for the next 20 years (Leahy J., 2016), have motivated the study of aircraft engine emissions and their related effects on the environment and human health. Several field and modelling studies have investigated the degradation of air quality near airports and have assessed the related effects on human health (e.g. Arunachalam et al. (2011), Barrett et al. (2013), Carslaw et al. (2006), Hsu et al. (2009), Lee et al. (2013) and Schürmman et al. (2007), among others). Aircraft engines are also a unique source of gases and particles in the upper troposphere and lower stratosphere, where they alter the atmospheric composition and contribute to climate change. In a study on the impacts of emissions from commercial aircraft flights on climate, Jacobson et al. (2013) reported that aircraft emissions were responsible for ~6 % of the Arctic surface global warming and ~1.3 % of total surface global warming. The radiative forcing from aircraft emissions results from the direct release of radiatively active compounds (greenhouse gases and particulate matter (PM)), species that produce or destroy radiatively active substances (e.g. nitrogen oxides (NO_x) as an ozone precursor), and species that trigger the formation of condensation trails and cirrus clouds (Penner et al., 1999). Of special interest are the aerosol-light interactions by strongly absorbing black carbon (BC), which are known to cause positive radiative forcing (i.e. warming). Although aviation BC emissions are very small relative to other anthropogenic sources like road transport, industry or biomass burning (Balkanski et al., 2010; Hendricks et al., 2004; Karagulian et al., 2017), their radiative effects can be enhanced when emitted at high altitude and over high surface albedo such as snow and ice surfaces or clouds. In fact, several model studies have shown that the direct radiation forcing (DRF) of BC strongly increases with altitude (e.g. Samset and Myhre, 2011; Zarzycki and Bond, 2010), and that globally, more than 40 % of the total DRF of BC is exerted at altitudes above 5 km (Samset et al., 2013). The presence of clouds is ~~are~~ a major contributor to the altitude dependency of the DRF of BC, but other factors such as surface albedo, water vapor concentrations and background aerosol distributions also contribute (Haywood and Shine, 1997; Samset and Myhre, 2011; Zarzycki and Bond, 2010). A detailed understanding of the optical properties of the carbonaceous particles emitted from aircraft exhaust is therefore essential to estimate the related climate effects.

Atmospheric PM scatters and absorbs solar radiation. Commonly reported optical parameters of PM include the absorption and scattering coefficients (b_{abs} and b_{scat}, respectively), and the single scattering albedo (SSA), defined as the ratio between light scattering and total extinction (absorption + scattering). The optical coefficients are often normalized to the

particle' mass to provide the mass absorption and mass scattering cross sections (MAC and MSC, respectively), which are essential parameters in atmospheric radiative transfer models. The MAC, MSC and SSA are key optical properties for the assessment of the aerosols radiative effects, and ~~strongly~~ depend on the particle size, morphology, and chemical composition. In the case of aircraft emissions, the characteristics of the PM emissions are influenced by the engine type, the thrust level (power) at which the engine is operated, and the fuel properties. The lack of experimental data on the optical properties of aircraft PM emissions has led to the extended use of generalized soot properties as an approximation to model aircraft radiative effects. This can lead to large discrepancies in the results, as the soot characteristics that determine the optical properties significantly vary among different combustion sources and combustion conditions. For example, aircraft soot particles are characterized by a very high degree of crystallinity and low oxidative reactivity (Liati et al., 2016; Parent et al., 2016), which might affect light absorption properties. In their meticulous review work, Bond and Bergstrom (2007) suggested a consistent MAC for fresh light-absorbing carbon ($MAC_{\lambda=550nm} = 7.5 \pm 1.2$ m^2 g^{-1}), independent of the combustion source or conditions. Higher MAC values were attributed to coating of the particles with negligibly-absorbing carbon. While in the size range of particles emitted from combustion processes the MAC stays nearly constant, the MSC has a strong dependency on the particle size (Hand and Malm, 2007), relative humidity (Khalizov et al., 2009), and coating with non-absorbing carbon (He et al., 2015). Levin et al. (2010) measured MSCs at 532 nm in the range 1.5 - 5.7 m^2 g^{-1} for fresh biomass burning smoke from a variety of fuels. In addition, a previous study of biomass burning emissions from Reid et al. (2005) reported a smaller range of MSC (3.2-4.2 m^2 g^{-1}) for fresh smoke, and larger MSC values for aged (coated) smoke (3.5-4.6 m^2 g^{-1}). Thus, while the MAC likely depends on the particles' chemical composition and morphology, the MSC (and SSA) have also a strong dependency on the particles' size. As indicated by our results, both the chemical composition and the particle size of aircraft fresh PM emissions largely vary with engine thrust. Therefore, the study of the thrust and fuel dependency of the radiative properties (MAC, MSC and SSA) of aircraft PM emissions is of key importance to decrease the uncertainty in the modelling of their radiative effects. ~~The strong dependency of MAC and MSC (and therefore SSA) on the particles` size, morphology and chemical composition (which as indicated by our results strongly varies with thrust), makes the measurement of the optical properties of aircraft PM emissions a key step to decrease the uncertainty in the modelling of their radiative effects.~~

Concerns of the limited reserves of fossil fuels and the environmental impacts of their consumption have led to the introduction of aviation biofuels. Compared to the standard Jet A-1 fuel, biofuels can have lower net CO_2 emissions. The use of biofuel blends in airliners is regulated by the ASTM D7566 (Standard specification for aviation turbine fuel containing synthesized hydrocarbons), which limits the maximum content of biofuel in the blend to 50% and sets restrictions to the blend aromatic content (minimum of 8%), lubricity, density, freezing point and viscosity (ASTM D7566-17a, 2017). One of the five ASTM certified blending components is biofuel from hydro-processed esters and fatty acids (HEFA), which can be produced from any form of fat or oil (e.g. waste fats from food industry or vegetable oils and fatty acids from oil/fat refining processes). The main difference between HEFA fuel and conventional Jet A-1 fuel is the absence of sulfur and aromatic species, commonly present in Jet A-1 in the range of 10-1000 ppm of sulfur and around 18% of aromatic content (Hadaller and Johnson, 2006). Previous works have shown that reducing sulfur and aromatics in the fuel decreases the sulfate and BC emissions, respectively

(Penner et al., 1999; Beyersdorf et al., 2014; Moore et al., 2015; Brem et al., 2015; Lobo et al., 2016). Moreover, a recent study on in-flight cruise emissions from the NASA DC-8 turbofan engines (CFM56-2-C1) has shown that using a 50:50 blend of Jet A and a Camelina-based HEFA biofuel ~~biofuel blends to power aircraft engines~~ reduces the ~~their~~ particle emissions by 50 - 70% (Moore et al., 2017).

In this work we study the link between the chemical composition and the optical properties of the PM measured at the engine exit plane of a CFM56-7B turbofan ~~from aircraft exhaust~~ for different engine loads and HEFA fuel blends. The measurements were performed using an in-service engine from the Boeing 737 Next Generation, which constitutes around 30% of all commercial airliners, and is therefore representative of the current fleet. The chemical characterization of the exhaust was based on the quantification ~~separation~~ of elemental and organic carbon (EC/OC analysis) from filter samples, while the optical properties were measured online at two different wavelengths. The resulting optical properties were then integrated in a simple two stream radiative model to estimate the direct forcing of fresh particle emissions from aircraft turbines during cruise conditions. The Simple Forcing Efficiency (SFE, Chylek and Wong, 1995) was evaluated over the entire solar spectrum for various surface albedos, including sea, grass, soil and snow. Complex models are required to model the atmospheric aging of the particles in the plume and to assess the radiative effects of the aged particles, which might significantly differ from those of the fresh emissions reported here.

2 Methods

2.1 Experimental set-up

The measurements were performed at the engine test cell of SR Technics at Zurich Airport (Switzerland) using an in-service commercial turbofan CFM56-7B burning four different blends of Jet A-1 and HEFA fuel (HEFA vol. percentage of 0, 5, 10, and 32%). A schematic of the experimental set-up is shown in Fig. 1. The exhaust was sampled at the engine exit plane using a single point sampling probe and then split into three sampling lines: the PM line for measurements of the particulate fraction, the GenTox line for the sampling of genotoxic compounds and the Annex 16 line for the measurements of the gaseous emissions and smoke number. The PM line was diluted with dry synthetic air (dilution factor ~ 1:10) to prevent water condensation and coagulation of the particles in the sampling line. The non-volatile PM (nvPM) measurement system is compliant with the new ICAO standard (ICAO, 2017). The instruments relevant for this work are shown in blue in Fig. 1. The chemical composition was determined from the analysis of filter samples with a Sunset OC-EC Aerosol Analyzer (Sunset Laboratory Thermal/Optical Carbon Analyzer, Model 4L). The optical properties were monitored online with a Photo-Acoustic Extinctiometer (PAX, Droplet Measurement Technologies, λ=870 nm) and a Cavity Attenuated Phase Shift PM single scattering albedo monitor (CAPS PM_{ssa}, Aerodyne, λ=532 nm). The particle size distribution was measured using a Scanning Mobility Particle Sizer (SMPS, TSI, Model 3938). The BC mass concentration was measured using a Micro-Soot Sensor (MSS, AVL, Model 483). The NO_2 measurement (Eco Physics, CLD844 S hr) was used to perform an online correction of the interference in the optical measurements at 532 nm. The CO_2 analyzers (Thermo Fisher Scientific Model 410i in the PM line

and Horiba PG-250 in the Annex 16 line) were used to calculate the dilution factors. Additional details of the measurement set-up are provided in the Supplementary Information (Sect. S1.1).

2.2 Filter samples for EC/OC analysis

Filter samples for EC/OC analysis were collected in the PM sampling line with a dual step stainless steel filter holder (URG, Series 2000-30FVT). Quartz fiber filters (Pall Tissuequartz, 2500QAT-UP) were used in both stages to collect the PM mass (main filter) and to determine the positive sampling artifact (back-up filter) from gaseous OC adsorbing onto the filter surface (Kirchstetter et al., 2000, Subramanian et al., 2004). Prior to sampling, the filters were baked for at least 6 hours at 650 °C to remove possible contaminations of adsorbed carbon. The sampling flow was 5 l min^{-1} and the duration was adjusted to provide optimal mass surface loadings for the EC/OC analyses (around 7 µg cm^{-2}). Stainless steel masks were deployed to reduce the sampling area of the filters and, as a result, increase the mass loading per sample area when needed. Overall, 16 sets of filters were collected to cover the full range of thrust levels for the Jet A-1 fuel and the 32% vol. HEFA blend. The larger filter masks (24 mm inner diameter) were used to sample at high thrust levels (100 - 65%), while the smaller masks (16 mm inner diameter) were required for the low thrust levels (50 - 7%).

The thermo-optical analysis for the quantification of EC and OC was performed using a Sunset OC-EC Aerosol Analyzer (Sunset Laboratory Thermal/Optical Carbon Analyzer, Model 4L). A detailed description of the method is reported in the Supplementary Information Sect. S1.2. For the analysis a modified NIOSH 5040 thermal protocol, summarized in Table S1 (Birch and Cary, 1996), with a transmittance optical correction for pyrolysis was used.

2.3 Measurement of the optical properties

The DMT PAX monitor simultaneously measures the aerosol optical absorption and scattering using a modulated diode laser (λ=870 nm). The light absorption is determined using the photo-acoustic technique. The modulated laser beam heats up the absorbing particles, which quickly transfer the heat to the surrounding air, generating a pressure wave that is measured with a sensitive microphone. The light scattering of the bulk aerosol is measured with a wide-angle integrating reciprocal nephelometer. Since there is relatively little absorption from gases and non-BC aerosol species at the 870 nm wavelength, the absorption measurement corresponds to the BC mass. Therefore, using an appropriate mass absorption cross section (MAC), the PAX absorption measurement can be used to determine BC mass (BC_{PAX}). Vice versa, comparing the absorption measurement with the EC mass from filter measurements, we can infer the MAC_{870} for aircraft engine exhaust.

The CAPS PM_{ssa} monitor provides simultaneous measurement of aerosols light extinction and scattering (Onasch et al., 2015). The extinction measurement is based on the cavity attenuated phase shift technique, which evaluates the phase shift of a LED light (532 nm) in a very long optical path (up to 2 km), created with very high reflectivity mirrors in the sampling cell (30 cm). In addition, the CAPS PM_{ssa} includes an integrating sphere (integrated nephelometer) within the optical path for the measurement of particle scattering. A particle size dependent truncation correction is required to take into account the light lost at extreme forward and backward scattering angles due to the apertures of the optical beam.

Laboratory calibrations of both instruments were performed prior to the measurement campaign using size selected ammonium sulfate and nigrosine PM (see Sect. S1.3 in the Supplementary Information). In addition to the standard calibrations, corrections for the CAPS scattering signal outside the instrument linear range and for the interference from gaseous NO_2 at the measurement wavelength were also developed (Fig. S2 and S3). While the measured NO_2 interference in the CAPS extinction is fairly consistent with previously reported values, we also found an unexpected non-linear interference in the CAPS scattering signal. This was initially attributed to a possible light leak in the instrument, but the scattering interference persisted after the light sealing of the instrument was renewed. To further investigate this issue, we compared laboratory calibration data of both optical instruments with results from Mie theory (Figs. S4-S6). Although there are several assumptions within the Mie model that may not be totally satisfied by the laboratory generated calibration particles (e.g. spherical and homogeneous particles), the agreement with the PAX absorption and scattering measurements is fairly good for both ammonium sulfate and nigrosine. In contrast, the CAPS measurements agree well with Mie theory only for purely scattering particles, i.e. ammonium sulfate. In the case of nigrosine, the CAPS measurements agree with Mie theory in terms of total extinction, but the measured scattering is around 43 % higher than estimated from the model. Despite several experimental efforts, we could not find the origin of the discrepancies in the CAPS scattering measurement or a way to properly correct it. Instead, we derived the CAPS scattering coefficient from the PAX absorption measurement using a thrust dependent absorption Angstrom exponent (AAE) obtained from aircraft engine measurements with a seven-wavelength aethalometer. All the details of this calculation can be found in Sect. S1.5 in the Supplementary Information.

2.4 Fuel specifications

The main differences between the conventional Jet A-1 fuel and the different HEFA blends used in this work are reported in Table 1. Most fuel properties were measured following the standard ASTM (American Society for Testing and Materials) methods, including the concentration of total aromatics, naphthalene and sulfur, the smoke point and the fuel density. In addition, the hydrogen mass concentration was determined by nuclear magnetic resonance, using a method equivalent to ASTM D7171. As expected, increasing the concentration of HEFA fuel in the blend corresponded to a reduction in the concentrations of the aromatic compounds (including ~~naphthalenes~~naphthalene) and sulfur. Besides, with the addition of the HEFA fuel the hydrogen mass concentration and the smoke point increased while the fuel density slightly decreased.

2.5 Radiative properties~~forcing~~

The SSA, MAC and MSC were calculated for the two measurement wavelengths (λ = 532 and 870 nm) using the following relationships:

$$SSA_\lambda = \frac{b_{scat,\lambda}}{b_{ext,\lambda}} \quad (1)$$

$$MAC_\lambda = \frac{b_{abs,\lambda}}{EC} \quad (2)$$

$$MSC_\lambda = \frac{SSA_\lambda * MAC_\lambda}{1-SSA_\lambda} \quad (3)$$

~~T~~In addition, to estimate the instantaneous direct radiative effects of the PM~~PM~~ from fresh aircraft engine exhaust, we evaluated the radiative transfer equation introduced by Chylek and Wong (1995), modified as in Bond et al. (2007), to express the wavelength dependent Simple Forcing Efficiency (SFE) in terms of the mass scattering coefficient (MSC) and the mass absorption coefficient (MAC):

$$SFE\ (\lambda) = -\frac{S_0(\lambda)}{4} T_{atm}^2(\lambda, z)(1-F_c)\left[2\left(1-a_s(\lambda)\right)^2 \beta(\lambda) MSC(\lambda) - 4a_s MAC(\lambda)\right], \quad (~~1~~4)$$

where S_0 is the top of the atmosphere solar irradiance, T_{atm} is the atmospheric transmission, F_c is the cloud fraction, a_s is the surface albedo, β is the backscatter fraction, λ is the wavelength, and z is the height over sea level.

~~To estimate the instantaneous direct radiative effects of the PM from aircraft engine exhaust we evaluated the radiative transfer equation introduced by Chylek and Wong (1995), modified as in Bond et al. (2007), to express the wavelength dependent Simple Forcing Efficiency (SFE) in terms of the mass scattering coefficient (MSC) and the mass absorption coefficient (MAC):~~

~~$SFE\ (\lambda) = -\frac{S_0(\lambda)}{4} T_{atm}^2(\lambda, z)(1-F_c)\left[2\left(1-a_s(\lambda)\right)^2 \beta(\lambda) MSC(\lambda) - 4a_s MAC(\lambda)\right]$, (1)~~

~~where S_0 is the top of the atmosphere solar irradiance, T_{atm} is the atmospheric transmission, F_c is the cloud fraction, a_s is the surface albedo, β is the backscatter fraction, λ is the wavelength, and z is the height over sea level.~~

The MAC and MSC determined for the two measurement wavelengths ~~(532 and 870 nm)~~ were fitted over the entire range of the solar radiation spectrum (280-4000 nm) using the power law relationships ~~in Eq. (2) and (3)~~:

$$MAC\ (\lambda) = a\lambda^{-AAE} \quad (~~2~~5)$$

$$MSC\ (\lambda) = b\lambda^{-SAE}, \quad (~~3~~6)$$

where a and b are fitting parameters, and AAE and SAE represent the absorption and scattering Angstrom exponents, respectively. The selection of the parameters in Eq. (~~1~~4) to (~~3~~6) ~~will be discussed in the results section~~are discussed in Sect. S2.4.

3 Results and discussion

All the results presented in this work were corrected to the engine exit plane taking into account the dilution in the PM line and the losses in the sampling system. The CO_2 measurements in the Annex 16 and the PM sampling lines were used to determine the dilution factor, and a size dependent correction was developed to estimate the diffusion and thermophoretic losses in the various sampling lines. Some additional considerations are needed regarding the representativeness of the data presented in this work. First, our results characterize the emissions at the engine exit plane from an engine operated ~~on~~ at the

ground. Thus, a correction to take into account the atmospheric conditions (temperature and pressure) at flight altitude is in principle necessary. However, as shown in Durdina et al. (2017) using data from a turbofan engine representative of modern commercial~~ly~~ engines (Howard et al., 1996), the altitude does not significantly influence the PM size distributions. While ambient conditions will affect the plume evolution, the effect on the PM chemistry at the engine exit plane can be assumed to be minimal. Consequently, also the optical properties, which strongly depend on the particle size and chemical composition, would remain unvaried at the engine exit plane. Hence we ~~can~~ assume the altitude correction for the optical properties at the engine exit plane to be negligible.~~minor as well.In addition,~~ It is important to note however, that most gaseous and particle species measured at the engine exit plane will rapidly evolve in the atmosphere and their radiative effects can largely vary from those of the direct emissions presented in this work, where the collected data correspond~~s~~ to a time after emission of approximately 0.1 to 0.6 seconds (Brem et al., 2015). Additional measurements are therefore required in order to assess the evolution of the particles' optical properties in the emission plume.~~the plume evolution of aircraft emissions in the atmosphere.~~ In any case, the emissions at the engine exit plane are the basis to consider the evolution of PM properties and are therefore the baseline for diverse atmospheric modelling scenarios.

3.1 Chemical composition ~~(EC/OC) analysis~~

An overview of the main findings from the EC/OC analysis is presented in Figs. 2 and 3. The OC concentrations were corrected to take into account the positive sampling artifact as described in the Supplementary Information (Sect. S2.1). The EC, OC and TC mass concentrations are reported in Table S3. Additionally, in Table S4 we also report the mass emission index of EC ($EI_{m,EC}$, in mg kg_{fuel}^{-1}), together with the additional parameters required for the calculation of EIs (i.e. carbon dioxide, carbon monoxide and hydrocarbon concentrations) and the particles' size parameters (geometric mean diameter (GMD) and geometric standard deviation (GSD)). Representative thermograms ~~containing~~ illustrating the EC/OC split for samples at low-, medium-, and high-thrust levels are reported in Fig. S9. ~~In Fig. 2, panels (a) (c) display~~

Figure 2 displays the mass concentrations of EC, OC and TC as a function of engine thrust ~~dependencies~~ and the concentration changes ~~in their concentrations~~ associated to the use of the 32% HEFA blend in comparison to the base Jet A-1 fuel. For the Jet A-1 fuel, the concentrations of all three carbonaceous components increased with engine thrust, from a minimum of 0.1 mgTC m^{-3} at taxi (~6% thrust) to a maximum of 5.6 mgTC m^{-3} at take-off (~95% thrust). As the mass concentration increased with thrust, the geometric mean diameter increased from 8 nm at taxi to 40 nm at take-off (Fig. S10). The slight increase in the mass concentrations between taxi and ground idle (~3% thrust) has been observed in previous works (Durdina et al., 2017) and is associated with a decrease in the combustion efficiency and the air/fuel ratio. As illustrated by the bar plots, ~~T~~the use of the 32% HEFA blend induced a clear reduction in the EC concentrations at all thrust levels, in line with previous findings (Moore et al., 2015~~, Brem et al., 2015~~; Moore et al., 2017; Schripp et al., 2018). The HEFA effect was strongest at low thrust levels, inducing a decrease in EC mass of 50-60% for thrust levels up to 30%. An explanation for this thrust dependence can be found in Brem et al. (2015). However, very large uncertainties were associated to the EC measurements at ground idle due to low filter loading (down to 0.2 µg cm^{-2} despite the long sampling times and the use of the

small filter mask). For thrust levels of 50% and above, the HEFA effect became less significant, reaching a minimum EC decrease of 14% at take-off. A similar trend was observed for the OC and TC concentrations at high thrust levels. In contrast, the OC, and consequently also the TC, seemed to be enhanced by the HEFA blend at ground idle.

~~Panels (d) and (e) in Fig. 2~~Figure 3 shows the correlations of EC and OC with the BC mass concentrations measured with the MSS (BC_{MSS}, reported as nvPM mass in regulatory measurements of aircraft engine emissions). EC and BC_{MSS} were in excellent agreement for both fuel types, with slope very close to unity (0.96 ± 0.02) and Pearson Coefficient (R^2) of 0.99. Although OC also increased with BC_{MSS}, the correlation was weaker in this case and small differences could be observed between the two fuels. ~~The fraction OC/TC reported in panel (f) showed a large variability with the thrust level, with OC/TC between 0.75 and 0.90 at low thrust levels (3 – 30%), decreasing to 0.25 at 50% thrust, and down to 0.17 at take-off. Similar trends in the OC/TC ratio with engine thrust have been observed in previous works (Delhaye et al., 2017). The use of the HEFA fuel did not have any visible effect on the OC/TC, but only on the concentrations.~~

3.2 Optical properties

The main results from the measurement of the optical properties are reported in Figs. ~~3~~4 and 5. For clarity, only the measurements with Jet A-1 fuel and the 32% HEFA blend are shown ~~in this plot~~, while the results from the intermediate HEFA blends (5% and 10%) are included in Fig~~s~~. S11 ~~and S12~~. ~~Panels (a) (e) in Fig. 3 report~~

Figure 4 presents the thrust dependencies of the absorption, scattering and extinction coefficients, measured at 532 nm (CAPS, green squares) and 870 nm (PAX, blue circles). At both wavelengths, b_{abs}, b_{scat} and b_{ext} showed ~~the same~~ similar thrust dependenci~~es~~ ~~as~~ to those observed for EC, characterized by a large and continuous increase for thrust levels above 40%. In addition, the use of the 32% HEFA blend induced a decrease in the three optical coefficients at most thrust levels. ~~At most thrust levels, the three optical coefficients decreased with the HEFA blend.~~

~~Panel (d)~~ Figure 5 shows the correlation between b_{abs} at the two measurement wavelengths and the EC mass concentration determined from the thermo-optical measurements. From the linear regressions we derive~~d~~d the MAC values for aircraft exhaust at 532 nm and 870 nm, which appear to be independent of the particle size distribution, thrust or ~~HEFA concentration~~fuel type, and will be further discussed in ~~the next s~~Section 3.4. The MAC_{870} was used to calculate BC mass from the PAX absorption measurement (BC_{PAX}), which was strongly correlated with BC_{MSS}. ~~BC_{PAX} and BC_{MSS} were strongly linearly correlated~~ (Fig. S12~~3~~, R^2 =0.99, slope 0.98) and showed thrust dependent reductions with the HEFA blends (Fig. S13), consistent with the reductions in EC mass.~~.~~

~~The decrease in both BC_{PAX} and BC_{MSS} with the 32% HEFA blend is illustrated in panel (e) in Fig. 3. While a decrease in the BC mass was observed already at low concentration blends for most thrust levels (Fig. S12), the largest effect was seen with the 32% HEFA blend. Similarly to the decrease in the EC mass (Fig. 2a), the decrease due to the 32% HEFA blend was highest at low thrust levels (e.g. at 6% thrust BC_{MSS} decreases by 74% and BC_{PAX} by 95%), while thrust levels above 60% were characterized by a lower and rather constant decrease (around 20% decrease in both BC measurements). The two instruments reported the same BC reduction at high thrust (high BC mass concentration), but disagreed increasingly as the BC mass~~

~~concentration decreased. This was attributed to the low sensitivity and high noise of the PAX at concentrations <10 µg m^{-3} relative to the MSS (error bars in panel (e)).~~

3.3. ~~The l~~Link between chemical composition and optical properties

To investigate the link between the chemical composition and the optical properties of the aircraft emissions, in Figure 6 we compare the thrust dependencies of the OC/TC fraction and the SSA, calculated at the two measurement wavelengths using Eq. (1). The ~~fraction~~ OC/TC fraction ~~reported in panel (f)~~ showed a large variability with the thrust level, with OC/TC between 0.75 and 0.90 at low thrust levels (3 - 30%), decreasing to 0.25 at 50% thrust, and down to 0.17 at take-off. Similar trends in the OC/TC ratio with engine thrust have been observed in previous works (Delhaye et al., 2017). Although the use of the HEFA fuel had a strong effect on the EC and OC mass concentrations, it did not have any visible effect on the OC/TC fraction. ~~The use of the HEFA fuel did not have any visible effect on the OC/TC, but only on the concentrations.~~

~~Lastly, panel (f) reports the SSA calculated at the two measurement wavelengths as the fraction of scattering to total extinction.~~ The high OC content of the particles at low thrust levels resulted in very high SSA, which showed a maximum at ground idle ($SSA_{~~CAPS~~532,base}$ = 0.88 and $SSA_{~~PAX~~870,base}$ = 0.55). Such high SSA values are common of particle emissions from biomass burning at low combustion efficiency (e.g. SSA_{532}~0.95 in wildfire emissions (Liu et al., 2014)). The SSA decreased sharply between 30% and 60% thrust, likely due to decreasing OC fraction~~. (Fig. 2f). The SSA was lowest~~ reaching a minimum at the combustor inlet temperatures and air/fuel ratios representative of cruise thrust (~60% thrust), where $SSA_{~~CAPS~~532,base}$ = 0.29 and $SSA_{~~PAX~~870,base}$ = 0.07. These low SSA values are characteristic of primary on-road vehicle particle emissions (e.g. 0.22 < SSA_{675} < 0.36 from tunnel measurements (Strawa et al., 2010)). Above 60% thrust ~~there wa~~we observed~~s~~ ~~again~~ a slight increase in the SSA, which might be related to the increasing mean particle size (as the OC content remained constant in this thrust range). While there was no visible effect from the HEFA blend at the~~se~~ high thrust levels, it seems that slightly higher SSA were associated to the HEFA blend at low thrust levels.

The similarities observed in the thrust dependencies of the OC/TC and the SSA, as well as the high correlation between BC_{PAX}, BC_{MSS} and EC, indicate that the OC content in these particles strongly enhanced light scattering at both measurement wavelengths, but did not have a substantial effect on the light absorption. The increased OC content of the PM with decreasing engine power is in agreement with the observations of Vander Wal et al. (2016), and could be explained by inefficient and incomplete combustion at the lower thrust levels. The thermograms from the EC/OC analysis show a large OC volatility range for all thrust levels, with a major fraction of OC evaporating between 200 and 310 °C, especially at low thrust (Fig. S9).

3.~~3~~ 4 Radiative properties~~forcing~~

~~For the calculation of the SFE defined in Eq. (1), $S_0(\lambda)$ (in W m^{-2} per nm of bandwidth) was set to the synthetic reference spectrum of solar irradiance at the top of the atmosphere developed by Gueymard (2004) (Fig. S14(a)). The wavelength dependent T_{atm} was evaluated for cruise conditions (z=12 km) using the Simple Model of the Atmospheric Radiative Transfer~~

~~of Sunshine (SMARTS) model (version 2.9.5, Gueymard, 2001), as detailed in the Supplementary Information (Sect. S2.4). Although previous works have proposed F_e = 0.6, Hassan et al. (2015) showed that Eq. (1) only performs properly when F_e is set to zero, while it gives unrealistic results when clouds are present. This is because the equation assumes that aerosols below or above clouds can be neglected, which is obviously incorrect and not supported by observations. Therefore, we only considered the case of F_e = 0. The surface spectral albedos "Water or calm ocean", "Perennial rye grass", "Light soil", and "Fresh dry snow" incorporated in the SMARTS model from the Jet Propulsion Laboratory Advanced Spaceborne Thermal Emission and Reflection Radiometer (ASTER) spectral reflectance database (Hook, 2018) were used to represent ground surfaces covered by sea water, grass, soil and snow, respectively. In absence of backscattering measurements, β was fixed to 0.17 as previously determined for highly absorbing soot (SSA = 0.2) from diesel emissions (Schnaiter et al., 2003).~~

~~The wavelength dependent MAC and MSC were determined by fitting the measurements with Eq. (2) and (3), as shown in Fig. S14(b).~~ The MAC values at the two measurement wavelengths were determined from the linear fits between ~~the~~ b_{abs} and ~~the~~ EC mass ~~(Fig. 3(d))~~, which yielded MAC_{532} = 7.5 ± 0.3 m^2 g^{-1} (R^2=0.97) and MAC_{870} = 5.2 ± 0.9 m^2 g^{-1} (R^2=0.94). As shown in Fig. 5, the MAC values appear to be independent of the thrust level and fuel type. The MAC_{870} ~~latter~~ is in good agreement with the filter based determined MAC value by Petzold and Schröder (1996) for jet engine aerosol (MAC_{800} = 6 m^2 g^{-1}), which using the inverse wavelength dependency of the cross section leads to $MAC_{870,calc}$ = 5.5 m^2 g^{-1}. ~~The~~ Our results are also in line with the MAC value of freshly generated light absorbing carbon proposed by Bond and Bergstrom (2007) (MAC_{550} = 7.5 ± 1.2 m^2 g^{-1}), which converted to the wavelengths of interest results in $MAC_{532,calc}$ = 7.8 ± 1.2 m^2 g^{-1} and $MAC_{870,calc}$ = 4.7 ± 0.8 m^2 g^{-1}.

The MSC values were calculated using its relation with the SSA and MAC reported in Eq. (3). In contrast to the MAC, the SSA, and consequently the MSC, were found to be highly thrust dependent., ~~i.e. SSA=MSC/(MSC+MAC).~~ Using the SSA measured at 60% thrust (SSA_{532} = 0.37 ± 0.03; SSA_{870} = 0.09 ± 0.01) and the MAC values reported above, this calculation yielded MSC_{532} = 4.5 ± 0.4 m^2 g^{-1} and MSC_{870} = 0.54 ± 0.04 m^2 g^{-1}. The MSC_{532}~~nm~~ falls within the higher end of MSCs measured for fresh biomass smoke by Levin et al. (2010). However, a more detailed comparison with literature values is hindered by the strong dependency of MSC on the particles size, morphology, and chemical composition.

The wavelength dependent MAC and MSC were determined by fitting the measurements with Eqs. (4) and (5), as shown in Fig. S14. The AAE in Eq. (~~2~~4) was set to 1.0 ± 0.2, as inferred for the BC emissions at cruise thrust level (60%) from the aethalometer measurements described in the Supplementary Information Sect. S1.5. This is a widely accepted value of AAE, often used in literature for fresh black carbon particles. Lastly, SAE = 4.5 ± 0.7 was calculated for cruise conditions using the scattering coefficients at the two measurement wavelengths, i.e. SAE = $\ln(b_{scat,532}/b_{scat,870})/\ln(532/870)$. To put these results in context, the obtained MAC and MSC spectra were used to estimate the direct radiative effect of fresh aircraft exhaust PM emissions during cruise, using the SFE defined in Eq. (1). A detailed description of the SFE model and its results can be found in the Supplementary Information Sect. S2.4; in the following we shortly discuss the main findings. For high surface albedo surfaces like snow, aircraft fresh PM emissions induced a strong warming effect (integrated $SFE_{450\text{-}2000,\ snow}$ = 4700 W g^{-1}). Other land surfaces, such as soil and grass, resulted in a more moderate warming ($SFE_{450\text{-}2000,\ soil}$ = 1500~~1600~~ W g^{-1} $SFE_{450\text{-}}$

$_{2000,\ grass}$ = ~~9~~800 W g^{-1}), while the effect of emissions over dark surfaces such as sea water was very low and with an overall cooling effect (SFE$_{450\text{-}2000,\ sea}$ = - ~~3~~90 W g^{-1}). However, these results need to be taken with caution, as this simple radiative model does not consider the effect of underlying clouds. Moreover, we only consider the effect of fresh PM emissions, corresponding to an approximate time after emission of less than 0.6 s, where the jet is still conserved and high temperatures prevent the condensation of volatile species. Previous studies have shown that sulfuric acid plays an important role in the formation of secondary PM in near-field aircraft plumes (Kärcher et al., 1996). Thus, plume evolution measurements of the particles' optical properties (if possible in-flight) and more complex models are needed to assess the overall radiative effects of aircraft PM emissions.

~~The SFE spectral dependence of the PM emissions during cruise conditions is shown in Fig. 4 for the four different ground types (i.e. surface albedos) considered in this work. Positive SFE indicates a warming effect; negative SFE corresponds to cooling. The high surface albedo of snow (a_{snow} = 0.5–1.0 for λ < 1400 nm), translated into a strong positive SFE, especially in the visible range. The highest spectral forcing over snow SFE_{snow} = 16.5 W g^{-1} nm^{-1} was found at the blue wavelength (450 nm). The lower surface albedos from grass and soil (on average a_s = 0.2 for both surface types) induced a moderate SFE, which even turned negative (i.e. cooling) at short wavelengths (λ< 400 nm for soil and λ < 490 nm for grass). However, the overall dominant effect was warming, with a maximum SFE of 2.6 W g^{-1} nm^{-1} found in the red visible range (between 700–760 nm) for both surface types. In contrast, the extremely low surface albedo from sea surfaces (a_{sea} = 0.004–0.04) yielded very small SFE, which was mainly negative and had a minimum of -1.7 W g^{-1} nm^{-1} at 330 nm. Figure 4 also contains the integrated forcing (in W g^{-1}) in the spectral range 450–2000 nm (limited by the availability of albedo data) for the four surface types. The strongest warming effect of the aircraft PM was observed when the emissions occurred above highly reflective surfaces like snow. The integrated SFE in this case was in the order of 4700 W g^{-1}. Other land surfaces (i.e. soil and grass) showed a moderate warming, with an integrated SFE in the range of 900 to 1600 W g^{-1}. The integrated effect of the emissions over dark surfaces like sea water was extremely low (~ -3 W g^{-1}) and, contrary to the other surface types, the overall effect was cooling.~~

~~This simple model does not consider the effects from underlying clouds. However, aircraft cruising altitude (10 – 13 km above sea level) normally exceeds the typical cloud top altitude (except in tropical latitudes). Samset and Myhre (2015) studied the differences in the modeled altitude dependence of the DRF of BC when clouds are taken into consideration, and found that globally the DRF of BC at cruise altitude (100 hPa) was doubled when using all-sky conditions (~2300 W g^{-1}) compared to clear-sky conditions (~1000 W g^{-1}). In a first approximation, we expect that cruise emissions above clouds will induce similar radiative effects to the emissions over snow-covered surfaces (i.e. strong warming), but more complex models are required to accurately determine the radiative effects of aircraft PM emissions.~~

4 Conclusions

This work presents the link between the EC/OC content and the optical properties of PM emissions at the engine exit plane of a CFM56-7B operated at a full range of thrust levels from ground idle to take-off. In addition, we examined the effects of using

HEFA biofuel blends on the PM emissions, - and determined the main radiative properties of the fresh PM emissions, which are of great value for the modelling of their radiative effects.

The EC and OC mass concentrations, as well as the absorption and scattering coefficients, increased with thrust level. While PM at the engine exit plane is thought to mostly contain strongly absorbing EC, we found a significant fraction of OC at low thrust levels, which was linked to the high scattering and SSA values. In line with previous studies, the 32% vol. HEFA blend significantly lowered the PM mass emissions, especially at low thrust levels, where the EC mass was reduced by 50-60%. The OC mass also decreased at most thrust levels, except at 3% thrust, where it seemed to be enhanced. However, at this thrust level we only had one sample for each fuel type, and the uncertainties attributed to these low thrust measurements with low concentrations were large.

The trends in the OC/TC ratio and the SSA highlighted important differences in the particles formed in the combustion process at different thrust levels. At low thrust levels, representative of ground idle and taxi, the particles were highly scattering (SSA_{532} = 0.7-0.9) and contained large fractions of OC (OC/TC = 0.75-0.9). In contrast, at the higher thrusts levels, representative of cruise (60% thrust) and take-off (100% thrust), the particles were composed mostly of highly absorbing EC (SSA_{532}= 0.3-0.4 and OC/TC = 0.2). The high OC fractions observed at low thrust levels are most probably a consequence of the lower efficiency of the combustion at these low engine powers. Regarding the use of HEFA blends, we could not see any significant effect from the different fuel types on the SSA and the OC/TC ratio.

The measurements of absorption and scattering at two different wavelengths, in combination with the measurements of EC mass, allowed us to evaluate the mass absorption and scattering cross sections (MAC and MSC) and to study their wavelength dependence. Together with the SSA, the MAC and MSC are key parameters for the study of the PM radiative effects. The obtained MAC was found to be independent of the thrust level and matched very well the values reported in literature for fresh BC. In contrast, the MSC (and SSA) varied greatly with thrust level, as it strongly depends on particle size, morphology and composition. As for the SSA, no effect was observed on the MAC and MSC from the use of the HEFA blends. Thus, the particles originated from the combustion of both fuel types seem to be equivalent in terms of their normalized optical properties and only their concentrations change. Previous works found significant differences in the morphology of the particles emitted when burning pure alternative fuels compared to standard jet fuels, which would translate into major differences in the particles' optical properties (Huang and Vander Wal, 2013; Huang et al., 2016). However, this does not seem to be the case for blends of alternative fuels at practical ratios for widespread usage in the foreseeable future and with considerable (> 8% v/v) total aromatics content. In fact, Huang and Vander Wal (2013) found similar trends in the soot nanostructure evolution with thrust for standard jet fuel and its 50:50 blend with an alternative fuel, while the two pure biofuels tested produced distinct and varied types of nanostructures independent of the engine thrust. Huang and Vander Wal (2013) related these differences to the different degrees of turbulent mixing in the combustion chamber prior to soot formation, which is linked to the aromatic content in the fuel. Thus, soot formation from blends with up to 50% of alternative fuel is fairly similar to the one of the unblended base fuel, which results in emissions of soot particles with similar morphology, OC/TC ratios and intensive optical properties.

The wavelength dependent MAC and MSC were used to estimate the instantaneous direct radiative forcing of fresh aircraft PM emissions during cruise conditions using a simple two stream model. Our results showed that in the absence of clouds, when the emissions occurred over dark surfaces like sea water, the forcing efficiency was very small and had a net cooling effect. In contrast, these particles had a strong warming effect when emitted above highly reflective surfaces, such as snow or ice. However, more accurate and complex climate models that simulate the atmospheric aging of the particles in the emission plume and take into account the effect from variable underlying cloud fields are required for a complete understanding of the impact of aviation particle emissions on the Earth's radiative balance.

~~Both scattering and absorption increased with thrust, as did the PM mass. However, the light scattering was dominant at low thrust levels, while absorption prevailed otherwise. These changes were reflected in the SSA, which varied extensively over the full thrust range, and was a critical parameter for the determination of the radiative effects. The variations in the optical behavior of the particles were linked to changes in the EC/OC content. While PM at the engine exit plane is thought to mostly contain strongly absorbing EC, we found a significant fraction of OC at low thrust levels, which explains the high scattering and SSA values.~~

~~In addition, we examined the effects of HEFA biofuel blends on the PM emissions. In line with previous studies, the 32% vol. HEFA blend significantly lowered the PM mass emissions, especially at low thrust levels, where the EC mass was reduced by 50-60%. The OC mass also decreased at most thrust levels, except at 3% thrust, where it seemed to be enhanced. However, at this thrust level we only had one sample for each fuel type, and the uncertainties attributed to these low thrust measurements with low concentrations were large. Moreover, we could not see any effect from using the HEFA blend on the intensive optical properties (i.e. SSA, MAC or MSC), nor on the EC/OC ratio. Thus, the particles originated from the combustion of both fuel types seem to be equivalent in terms of their normalized optical properties and only their concentrations change.~~

~~The combination of optical measurements at two wavelengths enabled us to evaluate the wavelength dependency of the optical properties, which is needed for the modeling of aerosol climate effects. For this purpose we used the SFE as an estimate of the instantaneous direct radiative forcing of the aircraft PM emissions during cruise conditions, and evaluated the differences among various surface albedos. In the absence of clouds, when the emissions occurred over dark surfaces like sea water, the forcing efficiency was very small and had a net cooling effect. In contrast, these particles had a strong warming effect when emitted above highly reflective surfaces, such as snow or ice. However, more accurate and complex climate models that include the effect from variable underlying cloud fields are required for a complete understanding of the impact of aviation particle emissions on the Earth's radiative balance.~~

Author contribution

ME designed the study, performed the laboratory calibrations and the data analysis. BTB and FS were in charge of fuel logistics. FS coordinated the test cell availability and engine lease. ME, BTB, LD and DS performed the jet engine

measurements. AF performed the EC/OC analysis. ME wrote the manuscript with important contributions from BTB, LD and AF. BTB, LD, AF and JW revised the manuscript.

Data availability

The numerical data used to make the figures in this manuscript and the corresponding supplementary information is available at https://doi.org/10.5281/zenodo.1918161 (Elser et al., 2018).

Competing interests

The authors declare that they have no conflict of interest.

Acknowledgements

Funding was provided by the Swiss Federal Office of Civil Aviation (FOCA) through the project SFLV 2015-113 "EMPAIREX – EMissions of Particulate and gaseous pollutants in AIRcraft engine EXhaust". We thank Mike Weiner and the test cell crew from SR Technics AG for operating the engine testing facility, our EMPA colleagues Regula Haag and Dr. Daniel Rentsch for the fuel hydrogen analysis, Dr. Michael Arndt from AVL GmbH for loaning the PAX instrument, and the group of Dr. André Prévôt from PSI for providing the Aethalometer data.

References

Arunachalam, S., Wang, B., Davis, N., Baek, B. H., and Levy, J. I.: Effect of chemistry transport model scale and resolution on population exposure to PM2.5 from aircraft emissions during landing and takeoff, Atmos. Environ., 45, 3294–3300, doi:10.1016/j.atmosenv.2011.03.029, 2011.

ASTM D7566-17a: Standard specification for aviation turbine fuel containing synthesized hydrocarbons, ASTM International, West Conshohocken, PA, 2017.

Balkanski, Y., Myhre, G., Gauss, M., Radel, G., Highwood, E.J., and Shine, K.P.: Direct radiative effect of aerosols emitted by transport: from road, shipping and aviation, Atmos. Chem. Phys., 10, 4477–4489, doi:10.5194/acp-10-4477-2010, 2010.

Barrett, S. R. H., Britter, R. E., and Waitz, I. A.: Impact of aircraft plume dynamics on airport local air quality, Atmos. Environ., 74, 247–258, doi:10.1016/j.atmosenv.2013.03.061, 2013.

Beyersdorf, A. J., Timko, M. T., Ziemba, L. D., Bulzan, D., Corporan, E., Herndon, S. C., Howard, R., Miake-Lye, R., Thornhill, K. L., Winstead, E., Wey, C., Yu, Z., and Anderson, B. E.: Reductions in aircraft particulate emissions due to the use of Fischer–Tropsch fuels, Atmos. Chem. Phys., 14, 11-23, doi:10.5194/acp-14-11-2014, 2014.

Birch, M. E., and Cary, R. A.: Elemental carbon-based method for monitoring occupational exposures to particulate diesel exhaust, Aerosol Sci. Technol., 25, 221–241, doi:10.1080/02786829608965393, 1996.

Bond, T. C., and Bergstrom R. W.: Light absorption by carbonaceous particles: An investigative review, Aerosol Sci. Tech., 40, 27-67, doi:10.1080/02786820500421521, 2007.

Brem, B. T., Durdina, L., Siegerist, F., Beyerle, P., Bruderer, K., Rindlisbacher, T., Rocci-Denis, S., Gurhan Andac, M., Zelina, J., Penanhoat, O., and Wang, J.: Effects of fuel aromatic content on nonvolatile particulate emissions of an in-production aircraft gas turbine, Environ. Sci. Technol., 49, 13149-13157, doi:10.1021/acs.est.5b04167, 2015.

Carslaw, D. C., Beevers, S. D., Ropkins, K., and Bell, M. K.: Detecting and quantifying aircraft and other on-airport contributions to ambient nitrogen oxides in the vicinity of a large international airport, Atmos. Environ., 40, 5424–5434, doi:10.1016/j.atmosenv.2006.04.062, 2006.

Chylek, P., and Wong, J.: Effect of absorbing aerosols on global radiation budget, Geophys. Res. Lett., 22, 929-931, doi: 10.1029/95GL00800, 1995.

Delhaye, D., Ouf, F.X., Ferry, D., Ortega, I.K., Penanhoat, O., Peillon, S., Salm, F., Vancassel, X., Focsa, C., Irimiea, C., Harivel, N., Perez, B., Quinton, E., Yon, J., and Gaffie, D.: The MERMOSE project: Characterization of particulate matter emissions of a commercial aircraft engine, J. Aerosol Sci., 105, 48-63, doi:10.1016/j.jaerosci.2016.11.018, 2017.

Durdina, L., Brem, B.T., Setyan, A., Siegerist, F., Rindlisbacher, T., and Wang, J.: Assessment of Particle Pollution from Jetliners: from Smoke Visibility to Nanoparticle Counting, Environ. Sci. Technol., 51, 3534-3541, doi:10.1021/acs.est.6b05801, 2017.

Elser, M., Brem, B. T., Durdina, L., Schönenberger, D., Siegerist, F., Fischer, A., and Wang, J.: Zenodo, Empairex 1: Optical properties data archive, doi:10.5281/zenodo.1918161, 2018.

~~Gueymard, C.: Parameterized transmittance model for direct beam and circumsolar spectral irradiance, Solar Energy, 71, 325-346, doi:10.1016/S0038-092X(01)00054-8, 2001.~~

~~Gueymard, C: The sun's total and spectral irradiance for solar energy applications and solar radiation models, Solar Energy, 76, 423-453, doi:10.1016/j.solener.2003.08.039, 2004.~~

Hadaller, O. J., and Johnson, J. M.: World Fuel Sampling Program, CRC Report 647, Coordinating Research Council, Inc., Alpharetta, GA, 2006.

Hand, J. L., and Malm, W. C.: Review of aerosol mass scattering efficiencies from ground-based meaurements since 1990, J. Geophys. Res., 112, D16203, doi:10.1029/2007JD008484, 2007.

~~Hassan T., Moosmueller, H., and Chung, C. E.: Coefficients of an analytical aerosol forcing equation determined with a Monte-Carlo radiation model, J. Quant. Spectrosc. Radiat. Transf., 164, 129-136, doi:10.1016/j.jqsrt.2015.05.015, 2015.~~

Haywood, J. M., and Shine, K. P.: Multi-spectral calculations of the direct radiative forcing of tropospheric sulphate and soot aerosols using a column model, Q. J. Roy. Meteor. Soc., 123, 1907-1930, doi:10.1002/qj.49712354307, 1997.

He, C., Liou, K.-N., Takano, Y., Zhang, R., Levy Zamora, M., Yang, P., Li, Q., and Leung, L. R.: Variation of the radiative properties during black carbon aging: theoretical and experimental intercomparison, Atmos. Chem. Phys., 15, 11967–11980, doi:10.5194/acp-15-11967-2015, 2015.

Hendricks, J., Karcher, B., Dopelheuer, A., Feichter, J., Lohmann, U., and Baumgardner, D.: Simulating the global atmospheric black carbon cycle: a revisit to the contribution of aircraft emissions, Atmos. Chem. Phys., 4, 2521–2541, doi:10.5194/acp-4-2521-2004, 2004.

~~Hook, S. J.: ECOSTRESS spectral library, Jet Propulsion Laboratory, California Institute of Technology, http://speclib.jpl.nasa.gov, last access: 26 April 2018.~~

Howard, R., Hiers, R.S., Whitefield, P. D., Hagen, D. E., Wormhoudt, J. C., Miake-Lye, R. C., and Strange, R.: Experimental characterization of gas turbine emissions at simulated altitude conditions, Arnold Engineering Development Center, AEDC-TR-96-3, 1996.

Hsu, H. H., Adamkiewicz, G., Houseman, E. A., Zarubiak, D., Spengler, J. D., and Levy, J. I.: Contributions of aircraft arrivals and departures to ultrafine particle counts near Los Angeles international airport, Sci. Total Environ., 444, 347–355, doi:10.1016/j.scitotenv.2012.12.010, 2013.

Hsu, S., Fruin, S., Kozawa, K., Mara, S., Winer, A. M., and Paulson, S. E.: Aircraft emission impacts in a neighborhood adjacent to a general aviation airport in Southern California, Environ. Sci. Technol., 43, 8039–8045, doi:10.1021/es900975f, 2009.

Huang, C.-H., and Vander Wal, R.L.,: Effect of soot structure evolution from commercial jet engine burning petroleum based JP-8 and synthetic HRJ and FT fuels, Energy Fuels, 27, 4946-4958, doi: 10.1021/ef400576c, 2013.

Huang, C.H., Bryg, V.M., and Vander Wal, R.L.: A survey of jet aircraft PM by TEM in APEX III, Atmos. Environ., 140, 614-622, doi:10.1016/j.atmosenv.2016.06.017, 2016.

ICAO: Annex 16 to the Convention on International Civil Aviation, Environmental Protection, Volume II Aircraft Engine Emissions, Fourth Edition, 2017.

Jacobson, M. Z., Wilkerson, J. T., Naiman, A. D., and Lele, S. K.: The effects of aircraft on climate and pollution. Part II: 20-year impacts of exhaust from all commercial aircraft worldwide treated individually at the subgrid scale, Faraday Discuss., 165, 369-382, doi:10.1039/C3FD00034F, 2013.

Karagulian, F., Van Dingenen, R., Belis, C.A., Janssens Maenhout, G., Crippa, M., Guizzardi, D., and Dentener, F.: Attribution of anthropogenic PM2.5 to emission sources, JRC Technical Reports, EUR 28510 EN, doi:10.2760/344371, 2017.

Kärcher, B., Hirschberg, M. M., and Fabian, P.: Small-scale chemical evolution of aircraft exhaust species at cruising altitudes, J. Geophys. Res., 101, 15169–15190, doi:10.1029/96JD01059, 1996.

Khalizov, A. F., Xue, H., Wang, L., Zheng, J., and Zhang, R.: Enhanced light absorption and scattering by carbon soot aerosol internally mixed with sulfuric acid, J. Phys. Chem. A., 113, 1066–1074, doi:10.1021/jp807531n, 2009.

Kirchstetter, T. W., Corrigan, C. E., and Novakov, T.: Laboratory and field investigation of the adsorption of gaseous organic compounds onto quartz, Atmos. Environ., 35, 1663-1671, doi:10.1016/S1352-2310(00)00448-9, 2001.

Leahy, J.: Airbus Global Market Forecast 2016-2035, 2016.

Lee, H., Olsen, S. C., Wuebbles, D. J., and Youn, D: Impacts of aircraft emissions on the air quality near the ground, Atmos. Chem. Phys., 13, 5505–5522, doi:10.5194/acp-13-5505-2013, 2013.

Levin, E. J. T., McMeeking, G. R., Carrico, C. M., Mack, L. E., Kreidenweis, S. M., Wold, C. E., Moosmüller, H., Arnott, W. P., Hao, W. M., Collett Jr., J. L., and Malm, W. C.: Biomass burning smoke aerosol properties measured during Fire Laboratory at Missoula Experiments (FLAME), J. Geophys. Res., 115, D18210, doi:10.1029/2009JD013601, 2010.

Liu, S., Aiken, A. C., Arata, C., Dubey, M. K., Stockwell, C. E., Yokelson, R. J., Stone, E. A., Jayarathne, T., Robinson, A. L., DeMott, P. J., and Kreidenweis, S. M: Aerosol single scattering albedo dependence on biomass combustion efficiency: Laboratory and field studies, Geophys. Res. Lett., 41, 742–748, doi:10.1002/2013GL058392, 2014.

Lobo, P., Condevaux, J., Yu, Z., Kuhlmann, J., Hagen, D.E., Miake-Lye, R.C., Whitefield, P.D., and Raper, D.W.: Demonstration of a Regulatory Method for Aircraft Engine Nonvolatile PM Emissions Measurements with Conventional and Isoparaffinic Kerosene fuels, Energy Fuels, 30, 7770–7777, doi: 10.1021/acs.energyfuels.6b01581, 2016.

Moore, R.H., Shook, M., Beyersdorf, A., Corr, C., Herndon, S., Knighton, W.B., Miake-Lye, R., Thornhill, K.L., Winstead, E.L., Yu, Z., Ziemba, L.D., and Anderson, B.E.: Influence of Jet Fuel Composition on Aircraft Engine Emissions: A Synthesis of Aerosol Emissions Data from the NASA APEX, AAFEX, and ACCESS Missions, Energy Fuels, 29, 2591–2600, doi:10.1021/ef502618w, 2015.

Moore, R. H., Thornhill, K. L., Weinzierl, B., Sauer, D., D'Ascoli, E., Kim, J., Lichtenstern, M., Scheibe, M., Beaton, B., Beyersdorf, A. J., Barrick, J., Bulzan, D., Corr, C. A., Crosbie, E., Jurkat, T., Martin, R., Riddick, D., Shook, M., Slover, G., Voigt, C., White, R., Winstead, E., Yasky, R., Ziemba, L. D., Brown, A., Schlager, H., and Anderson, B. E.: Biofuel blending reduces particle emissions from aircraft engines at cruise conditions, Nature, 543, 411–415, doi:10.1038/nature21420, 2017.

Onasch, T., Massoli, P., Kebabian, P., Hills, F., Bacon, F., and Freedman, A.: Single scattering albedo monitor for airborne particulates, Aerosol Sci. Technol., 49, 267-279, doi:10.1080/02786826.2015.1022248, 2015.

Penner, J. E., Lister, D. H., Griggs, D. J., Dokken, D. J., and McFarland, M.: Aviation and the global atmosphere. A special report of IPCC working groups I and III, Intergovernmental Panel on Climate Change, 1999.

Petzold, A., and Schröder, F. P.: Jet Engine Exhaust Aerosol Characterization, Aerosol Sci Technol., 28, 62-76, doi:10.1080/02786829808965512, 1998.

Reid, J. S., Eck, T. F., Christopher, S. A., Koppmann, R., Dubovik, O., Eleuterio, D. P., Holben, B. N., Reid, E. A., and Zhang, J.: A review of biomass burning emissions part III: Intensive optical properties of biomass burning particles, Atmos. Chem. Phys., 5,827–849, doi:10.5194/acp-5-827-2005, 2005.

Samset, B. H., and Myhre, G.: Vertical dependence of black carbon, sulphate and biomass burning aerosol radiative forcing, Geophys. Res. Lett., 38, L24802, doi:10.1029/2011GL049697, 2011.

Samset, B. H., Myhre, G., Schulz, M., Balkanski, Y., Bauer, S., Berntsen, T. K., Bian, H., Bellouin, N., Diehl, T., Easter, R. C., Ghan, S. J., Iversen, T., Kinne, S., Kirkevåg, A., Lamarque, J.-F., Lin, G., Liu, X., Penner, J. E., Seland, Ø., Skeie, R. B.,

Stier, P., Takemura, T., Tsigaridis, K., and Zhang, K.: Black carbon vertical profiles strongly affect its radiative forcing uncertainty, Atmos. Chem. Phys., 13, 2423-2434, doi:10.5194/acp-13-2423-2013, 2013.

~~Samset, B. H., and Myhre, G.: Climate response to externally mixed black carbon as a function of altitude, J. Geophys. Res. Atmos., 120, 2913–2927, doi:10.1002/2014JD022849, 2015.~~

~~Schnaiter, M., Horvath, H., Mohler, O., Naumann, K. H., Saathoff, H., and Schock, O. W.: UV-VIS-NIR spectral optical properties of soot and soot-containing aerosols, J. Aerosol Sci., 34, 1421–1444, doi:10.1016/S0021-8502(03)00361-6, 2003.~~

Schripp, T., Anderson, B., Crosbie, E.C., Moore, R.H., Herrmann, F., Oßwald, P., Wahl, C., Kapernaum, M., Köhler, M., Le Clercq, P., Rauch, B., Eichler, P., Mikoviny, T., and Wisthaler, A.: Impact of Alternative Jet Fuels on Engine Exhaust Composition During the 2015 ECLIF Ground-Based Measurements Campaign, Environ. Sci. Technol., 52, 4969-4978, doi:10.1021/acs.est.7b06244, 2018.

Schürmann, G., Schäfer, K., Jahn, C., Hoffmann, H., Bauerfeind, M., Fleuti, E., and Rappenglück, B.: The impact of NOx, CO and VOC emissions on the air quality of the airport Zurich, Atmos. Environ., 41, 103–18, doi:10.1016/j.atmosenv.2006.07.030, 2007.

Strawa, A., Kirchstetter, T. W., Hallar, A. G., Ban-Weiss, G. A., McLaughlin, J. R., Harley, R. A., and Lunden, M. M.: Optical and physical properties of primary on-road vehicle particle emissions and their implications for climate change, J. Aerosol Sci., 41, 36-50, doi:10.1016/j.jaerosci.2009.08.010, 2010.

Subramanian, R., Khlystov, A. Y., Cabada, J. C., and Robinson, A. L.: Positive and negative artifacts in particulate organic carbon measurements with denuded and undenuded sampler configurations, Aerosol Sci. Technol., 38, 27–48, doi: 10.1080/02786820390229354, 2004.

Vander Wal, R. L., Bryg, V. M., and Huang, C.-H.: Chemistry characterization of jet aircraft engine particulate matter by XPS: Results from APEX III, Atmos. Environ., 140, 623-629, doi:10.1016/j.atmosenv.2016.05.039, 2016.

Zarzycki, C. M., and Bond, T. C.: How much can the vertical distribution of black carbon affect its global direct radiative forcing?, Geophys. Res. Lett., 37, L20807, doi:10.1029/2010GL044555, 2010.

Property (units)	**Method**	**Jet A-1**	**HEFA 5%**	**HEFA 10%**	**HEFA 32%**
Aromatics (% v/v)	ASTM D 1319	18.1	17.1	16.2	11.3
Naphthalenes (% v/v)	ASTM D 1840	0.79	N.A.	N.A.	0.53
Sulfur (ppm)	ASTM D 5453	490	N.A.	N.A.	350
Hydrogen mass (% m/~~/~~m)	NMR	13.61~~13.8~~	13.68~~13.75~~	13.75~~13.81~~	14.09~~14.3~~
Smoke point (mm)	ASTM D 1322	22	N.A.	N.A.	24
Density (kg m^{-3})	ASTM D 4052	794.8	793.3	791.2	781.8

Table 1. Fuel specifications overview (N.A.: measurement not available)

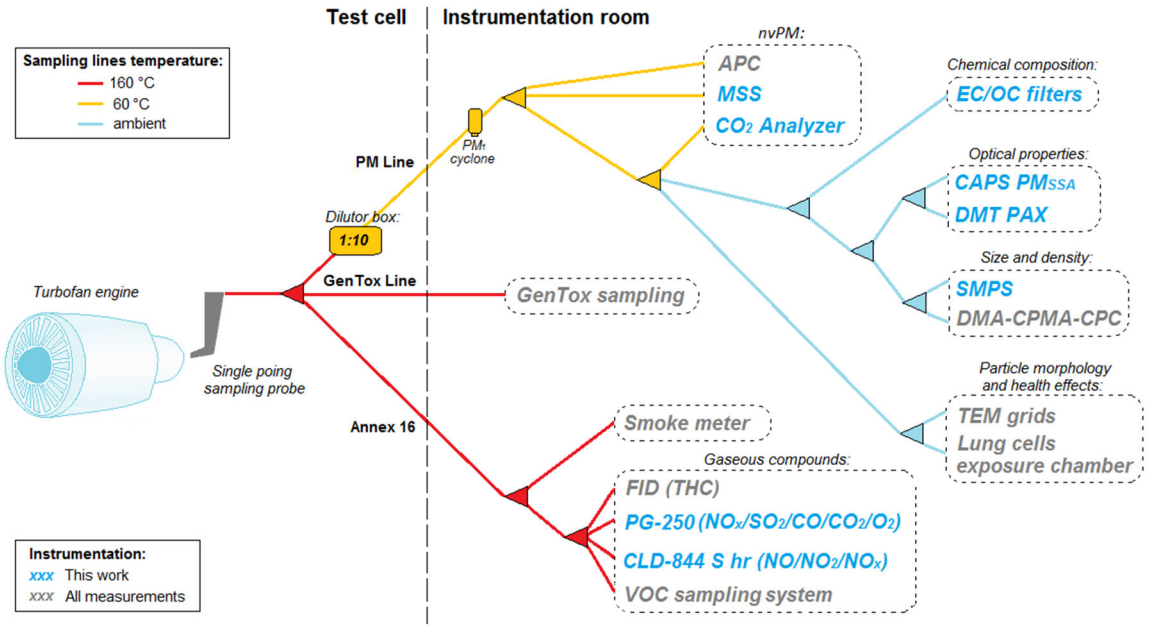

Figure 1: Experimental setup during EMPAIREX 1. Instruments depicted in blue were used in this work, which included: a Micro Soot Sensor (MSS), a Cavity Attenuated Phase-Shift Single Scattering Monitor (CAPS PM_{SSA}), a Photo Acoustic Extinctiometer (DMT PAX), a Scanning Mobility Particle Sizer (SMPS), a CO_2 analyzer, a Portable Multi Gas Analyzer (PG-250), and a Chemiluminescence Detector (CLD-844). Additional instrumentation that was not used in this work (depicted in grey) is described in the supplementary information (Sect. S1.1).

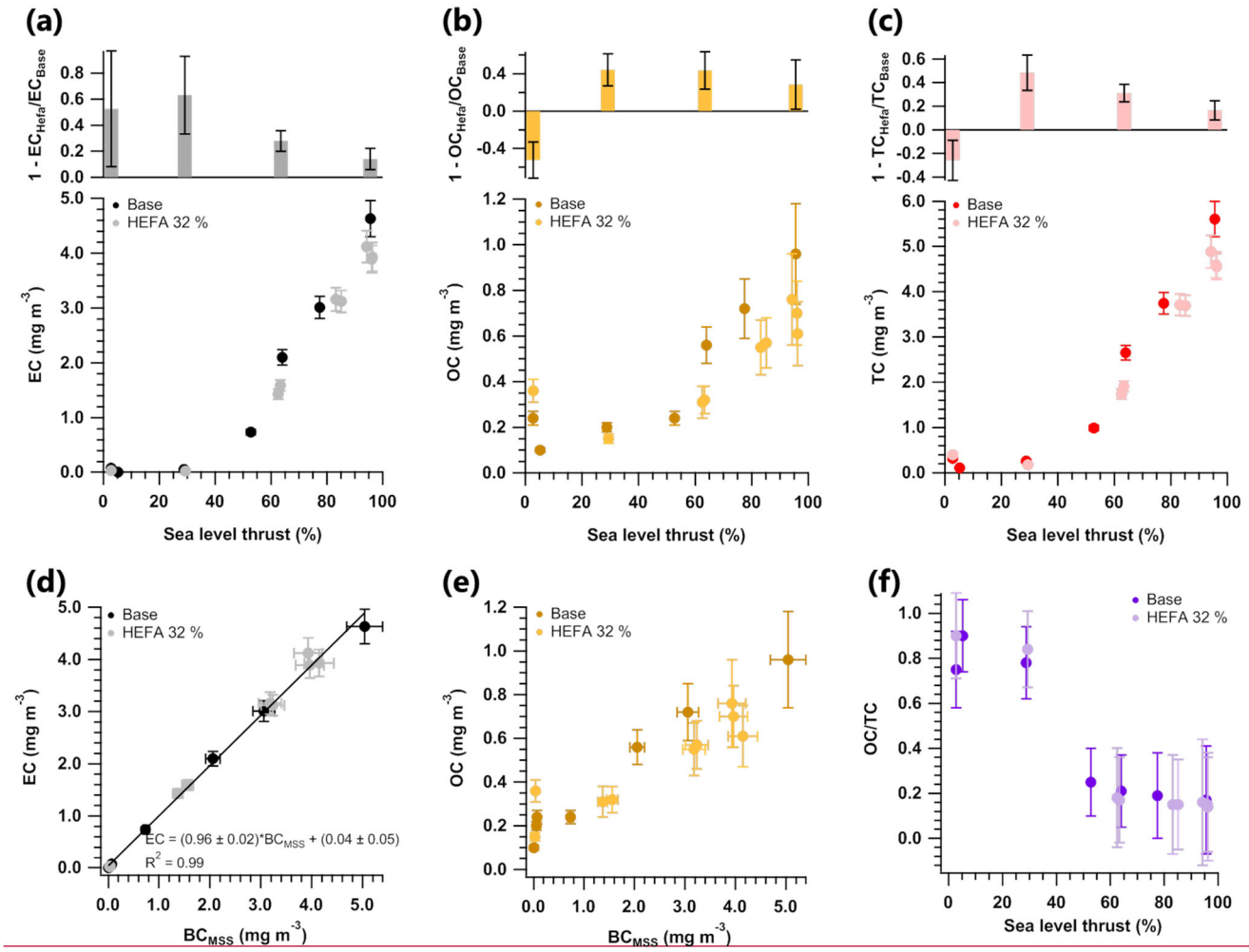
(a)
1 - EC_Hefa/EC_Base
EC (mg m-3)
Base
HEFA 32 %
Sea level thrust (%)
(b)
1 - OC_Hefa/OC_Base
OC (mg m-3)
Base
HEFA 32 %
Sea level thrust (%)
(c)
1 - TC_Hefa/TC_Base
TC (mg m-3)
Base
HEFA 32 %
Sea level thrust (%)
(d)
EC (mg m-3)
Base
HEFA 32 %
EC = (0.96 ± 0.02)*BC_MSS + (0.04 ± 0.05)
R2 = 0.99
BC_MSS (mg m-3)
(e)
OC (mg m-3)
Base
HEFA 32 %
BC_MSS (mg m-3)
(f)
OC/TC
Base
HEFA 32 %
Sea level thrust (%)

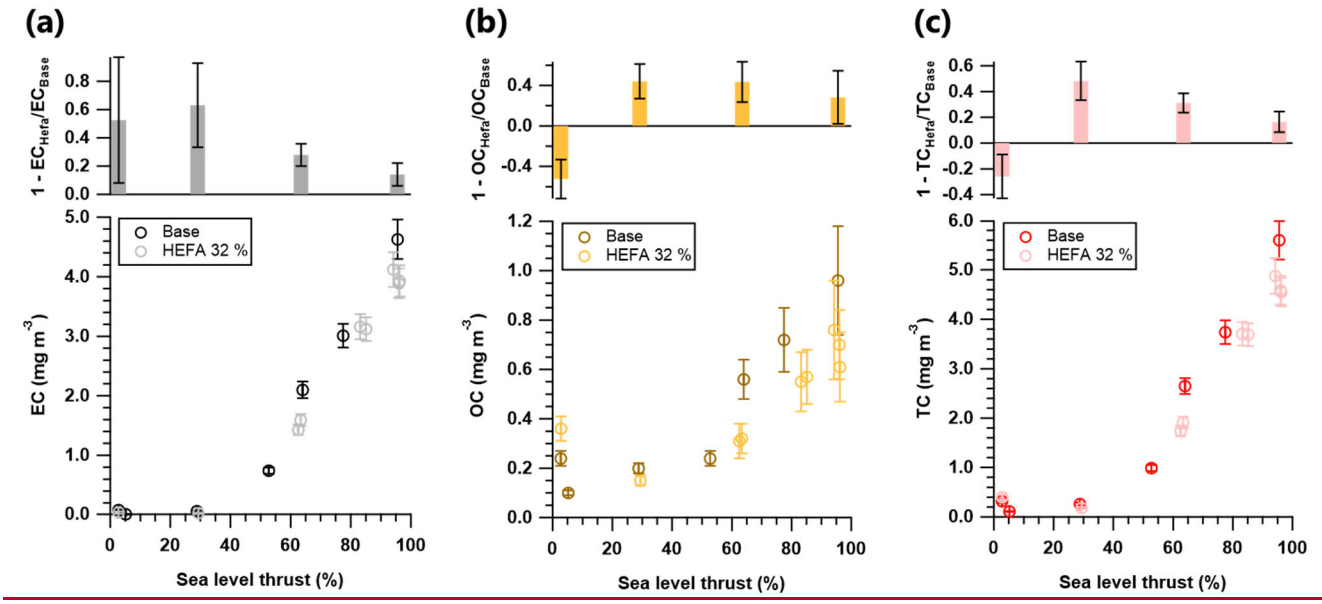

Figure 2. Thrust dependent mass concentration and decrease with the 32% HEFA blend compared to the base Jet A-1 fuel of (a) EC, (b) OC, and (c) TC. ~~**(d): Linear fit between EC and BC_{MSS} mass concentration. (e) Correlation between OC and BC_{MSS} mass concentration. (f): Thrust dependent OC to TC ratio.**~~ **Note: Dark colors represent measurements with base fuel (Jet A-1) and light colors represent measurements with the HEFA blend (32% vol.).**

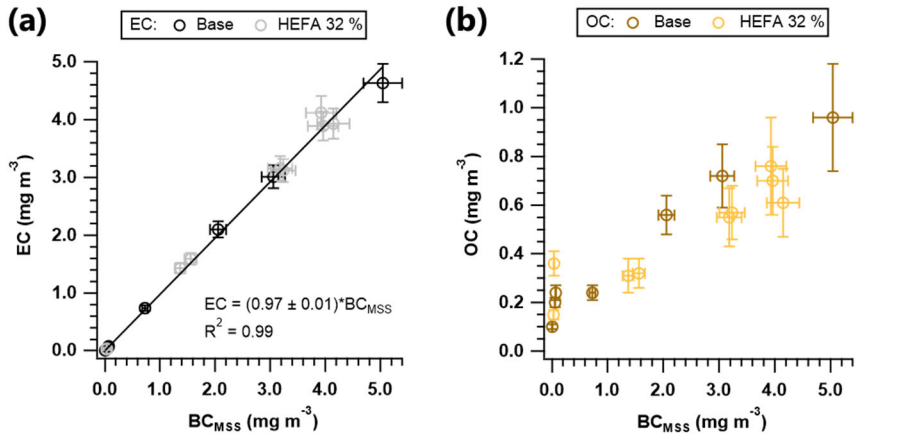

Figure 3. Correlation between the mass concentration of (a) EC, and (b) OC with BC_{MSS}. Note: Dark colors represent measurements with base fuel (Jet A-1) and light colors represent measurements with the HEFA blend (32% vol.).

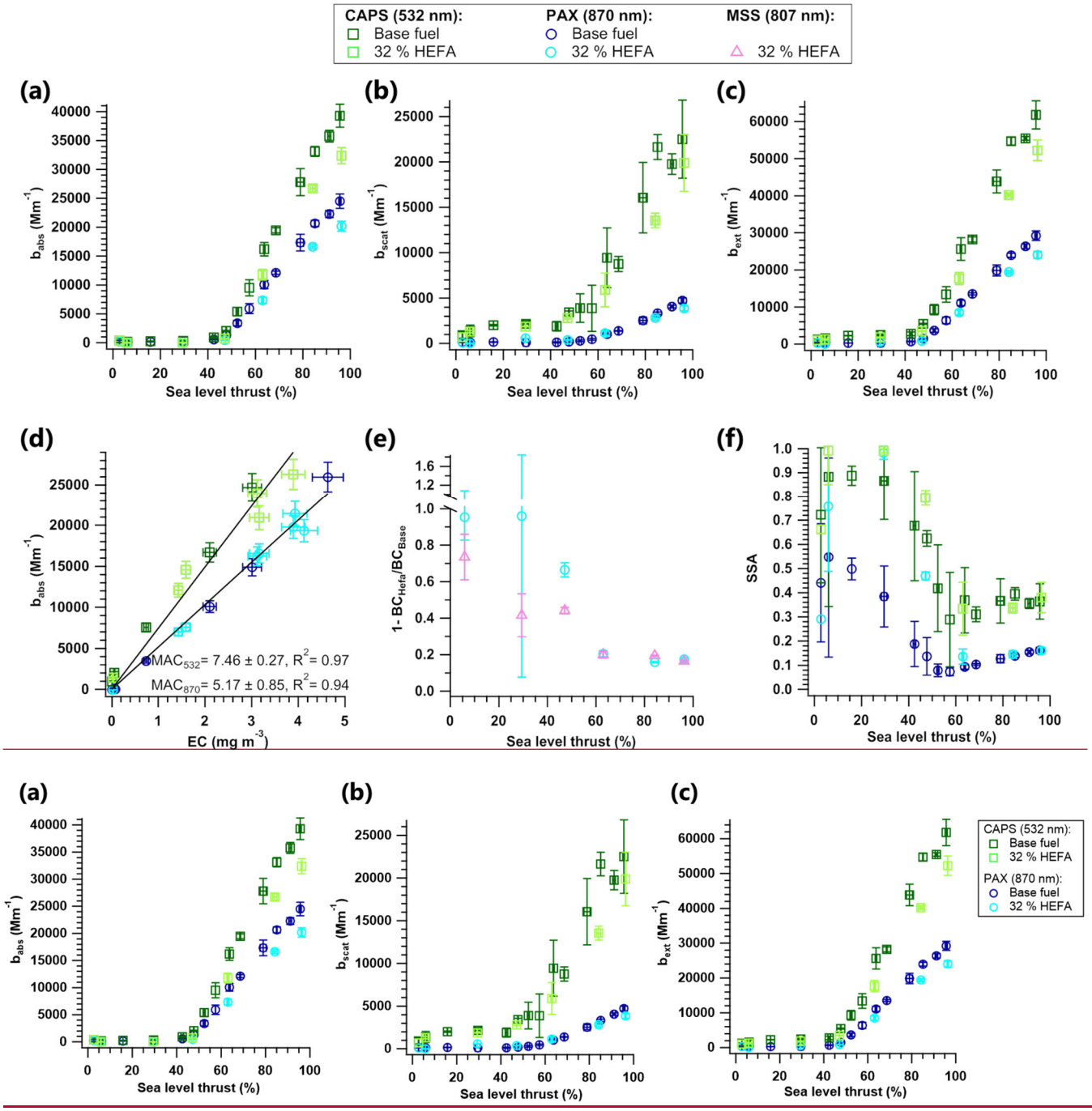

Figure 43. Thrust dependent (a) absorption, (b) scattering, and (c) extinction coefficients measured at 532 nm (green squares) and 870 nm (blue circles). ~~**(d) Correlation between the absorption coefficients and the EC mass concentration; MAC values are retrieved from the slope of the linear fits. (e) Thrust dependent decrease in BC_{MSS} and BC_{PAX} for the 32% HEFA blend in comparison to the base Jet A-1 fuel. (f) Thrust dependent single scattering albedo (SSA) at the two measurement wavelengths.**~~ **Note: Dark colors represent measurements with base fuel (Jet A-1) and light colors represent measurements with the 32% vol. HEFA blend.**

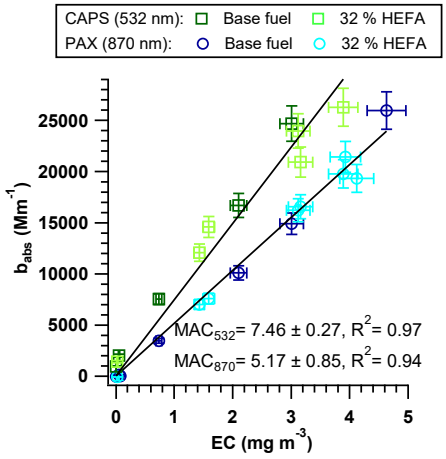

Figure 5. Correlation between the absorption coefficients measured at 532 nm (green squares) and 870 nm (blue circles) and the EC mass concentration; MAC values are retrieved from the slope of the linear fits. Note: Dark colors represent measurements with base fuel (Jet A-1) and light colors represent measurements with the HEFA blend (32% vol.).

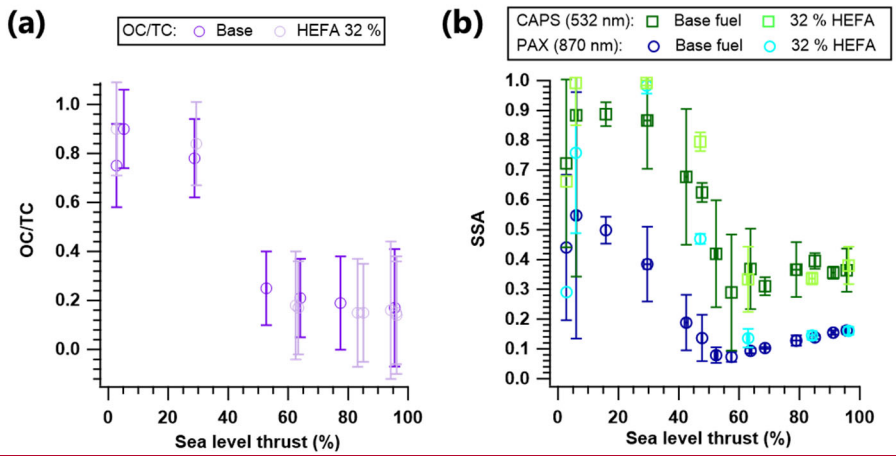

Figure 6. Thrust dependent (a) OC to TC ratio, and (b) SSA measured at 532 nm (green squares) and 870 nm (blue circles). Note: Dark colors represent measurements with base fuel (Jet A-1) and light colors represent measurements with the HEFA blend (32% vol.).

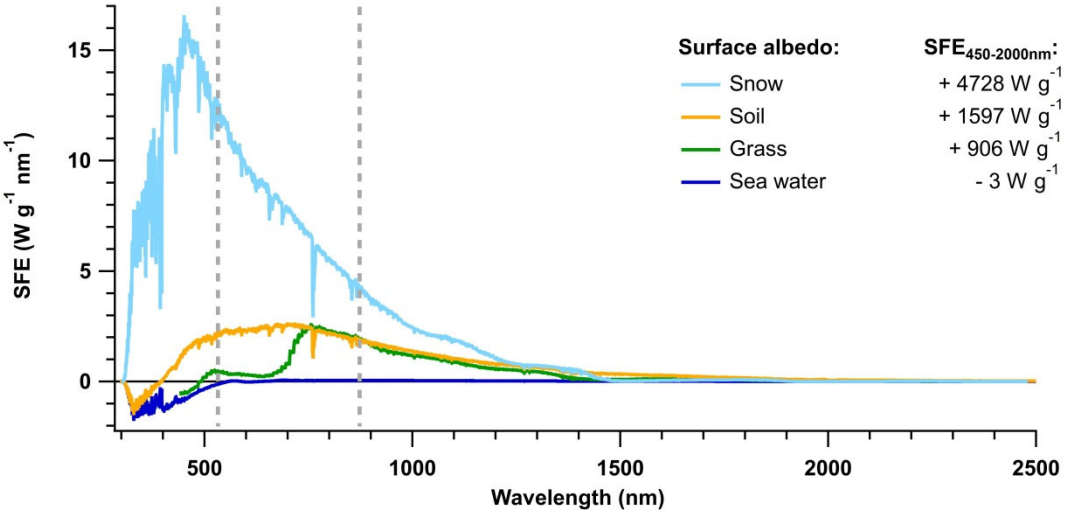

~~**Figure 4. Simple forcing efficiency (SFE) spectra for aircraft engine PM over different surface types, including sea water, grass, soil and snow, and integrated spectral values for the four surface types.**~~